DOI: 10.1002/chem.201103685

Bifunctional Rhenium Complexes for the Catalytic Transfer-Hydrogenation Reactions of Ketones and Imines

Anne Landwehr, Balz Dudle, Thomas Fox, Olivier Blacque, and Heinz Berke*[a]

Abstract: The silyloxycyclopentadienyl hydride complexes $[Re(H)(NO)(PR_3)(C_5H_4OSiMe_2tBu)]$ (R = *i*Pr (**3a**), Cy (**3b**)) were obtained by the reaction of $[Re(H)(Br)(NO)(PR_3)_2]$ (R = *i*Pr, Cy) with $Li[C_5H_4OSiMe_2tBu]$. The ligand–metal bifunctional rhenium catalysts $[Re(H)(NO)(PR_3)(C_5H_4OH)]$ (R = *i*Pr (**5a**), Cy (**5b**)) were prepared from compounds **3a** and **3b** by silyl deprotection with TBAF and subsequent acidification of the intermediate salts $[Re(H)(NO)(PR_3)(C_5H_4O)][NBu_4]$ (R = *i*Pr (**4a**), Cy (**4b**)) with NH_4Br. In nonpolar solvents, compounds **5a** and **5b** formed an equilibrium with the isomerized *trans*-dihydride cyclopentadienone species $[Re(H)_2(NO)(PR_3)(C_5H_4O)]$ (**6a,b**). Deuterium-labeling studies of compounds **5a** and **5b** with D_2 and D_2O showed H/D exchange at the H_{Re} and H_O positions. Compounds **5a** and **5b** were active catalysts in the transfer hydrogenation reactions of ketones and imines with 2-propanol as both the solvent and H_2 source. The mechanism of the transfer hydrogenation and isomerization reactions was supported by DFT calculations, which suggested a secondary-coordination-sphere mechanism for the transfer hydrogenation of ketones.

Keywords: bifunctional catalysts · homogeneous catalysis · hydrides · rhenium · transfer hydrogenation

Introduction

Ligand–metal bifunctional catalysis is an efficient method for the hydrogenation of various unsaturated organic compounds. Since Shvo and Czarkie reported that dinuclear precatalyst $[(\{2,3,4,5\text{-}Ph_4(\eta^5\text{-}C_4CO)\}_2H)Ru_2(CO)_4(\mu\text{-}H)]$[1] catalyzed the hydrogenation reactions of alkenes, alkynes,[2] imines,[3] and carbonyl compounds,[4] a number of catalysts with similar ligand environments have been demonstrated to accomplish related transformations.[5] In 1995, Noyori and co-workers discovered a highly efficient catalyst with excellent chemo- and enantioselectivities that exhibited "bifunctionality" of the transferred hydrogen atoms with hydridic H_{Ru} atoms and acidic H_N atoms on the chiral diamine ligands.[6] The mechanism of the hydrogen transfers of Shvo-type catalysts is a matter of controversy. Two plausible mechanisms have been suggested based on mechanistic experiments and DFT calculations.[3b,4a,7] Casey et al. proposed hydrogen transfer without pre-coordination of the substrate, the so-called "secondary-coordination-sphere mechanism",[3b,4a] whereas Bäckvall suggested a pre-coordination of the substrate to the metal center that was initiated by (η^4–η^3) ring-slippage of a π ligand before the hydrogen-transfers occurred in the primary coordination sphere.[7b]

[a] A. Landwehr, Dr. B. Dudle, Dr. T. Fox, Dr. O. Blacque, Prof. Dr. H. Berke
Institute of Inorganic Chemistry, University of Zurich
Winterthurerstrasse 190, 8057 Zurich (Switzerland)
Fax: (+41) 446354806
E-mail: hberke@aci.uzh.ch

Supporting information for this article is available on the WWW under http://dx.doi.org/10.1002/chem.201103685.

It was interesting to see whether the bifunctional property of heterolytically split H_2 (formally into H^- and H^+)[8] could be retained by isoelectronic substitution at the ruthenium center, thereby leaving the hydroxy cyclopentadienyl group as a proton donor but replacing the hydridic moiety of H-Ru-CO with the isoelectronic H-Re-NO unit. Realization of this goal seemed feasible, because the acidic hydrogen atom appeared to be grossly transition-metal independent and the hydridic hydrogen atom was anticipated to be tunable by the ligand sphere and adjustable in the hydridic character required for proper transfer reactivity. Certain geometric restraints were expected to arise for "bifunctional" H transfer, but principally these restrictions seemed to also be tunable within a certain range. Recently, complexes with rhodium,[9] iridium,[9b,10] osmium,[11] iron,[7a,c,12] tungsten,[13] and rhenium[14] centers have been reported to accomplish related bifunctional reactivity. $[Re(NO)(L)(H)(C_5H_4OH)]$ complexes, which are analogous to Shvo systems, were sought as targets where L was envisaged to be a $2e^-$ donor, such as CO or a monodentate phosphine group.

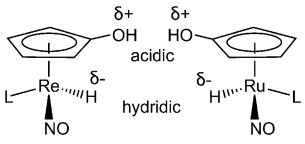

The only reported bifunctional rhenium complex to operate along the lines of bifunctional catalysis was described by Gusev and co-workers. However, the $[Re\text{-}H(NO)\{N(C_2H_4PiPr_2)_2\}]$ system, which is a Noyori-type cata-

lyst with an acidic amine group, revealed low catalytic performance.[14] Several rhenium–nitrosyl complexes have shown much-better catalytic performance in hydrosilylation[15] and hydrogenation reactions,[15a,16] which confirmed the high affinity of rhenium towards hydrogen and its general ability to drive catalytic hydrogenation cycles. Herein, we report the synthesis and reactivity of the first rhenium-based Shvo-type bifunctional $[Re(H)(NO)(PR_3)(C_5H_4OH)]$ compounds and we probe their catalytic performance in the transfer hydrogenation of ketones and imines by using 2-propanol as a hydrogen donor. Such transfer-hydrogenation catalysis seemed feasible on the basis of the existence of hydrogen-enriched and hydrogen-depleted forms.

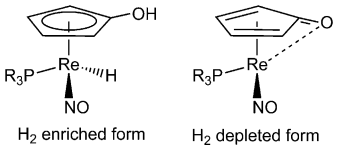

Similar to the Shvo system, the hydrogen-depleted form was envisaged to be a $16e^-$ cyclopentadienone–rhenium complex, which was perhaps further stabilized by weak O_{CO} coordination. Both forms differed in the rhenium redox states: rhenium(I) versus rhenium(−I). The accessibility of these states seemed feasible in view of the generally high disposition of rhenium towards redox changes, such as the Re^{I}/Re^{III} changes in the already mentioned hydrogenation and hydrosilylation reactions.[15b,16a,c] In addition, provided that the protonic/hydridic polarization of the hydrogen-enriched form and the secondary-coordination-sphere geometry for the $H(\delta^-)/H(\delta^+)$ atom-transfers are not too different for ruthenium and rhenium, effective bifunctional catalysis could indeed be expected to result from this simple Ru−CO/Re−NO replacement.

Results and Discussion

We wanted to synthesize the target $[Re(H)(NO)(PR_3)(C_5H_4OH)]$ complexes through the "late" stage introduction of the hydroxycyclopentadienyl ligand, once all of the other ligands (hydride, phosphine, and NO ligands) had been introduced into the coordination sphere of rhenium. The synthesis of suitable starting complexes of the type $[Re(H)(Br)(NO)(PR_3)_2]$, which contained these three "fixed" ligands and other replaceable moieties, has been reported by ourselves previously.[15b] The hydroxycyclopentadienyl moiety needed to be introduced into the rhenium coordination sphere in its silyl-protected form to prevent oxygen-coordination to the rhenium center (Scheme 1).

Preparation of complexes $[Re(H)(NO)(PR_3)(C_5H_4OSiMe_2tBu)]$ (3a and 3b): The $16e^-$ rhenium–hydride complexes $[Re(H)(Br)(NO)(PR_3)_2]$ (R = *i*Pr (**1a**), Cy (**1b**)) were reacted with (*tert*-butyldimethylsiloxy)cyclopentadienyl lithium (**2**) to accomplish the substitution of one phosphine ligand and the bromide ligand. At room temperature in THF, these reactions afforded the desired $[Re(H)(NO)(PR_3)(C_5H_4OSiMe_2tBu)]$ products (**3a** (R = *i*Pr), **3b** (R = Cy)) as orange oils in 92% (**3a**) and 86% (**3b**) yield.

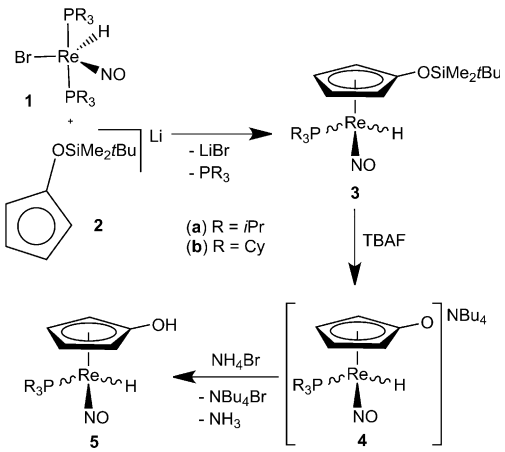

Scheme 1. Synthesis of $[Re(H)(NO)(PR_3)(C_5H_4OH)]$ complexes **5a** and **5b**.

Compounds **3a** and **3b** were fully characterized by IR and NMR spectroscopy, MS, as well as by elemental analysis and X-ray diffraction. The ^1H NMR spectra exhibited characteristic doublets for the hydride ligands of compound **3a** ($\delta = -9.01$ ppm, $^2J(H,P) = 28.1$ Hz) and compound **3b** ($\delta = -8.97$ ppm, $^2J(H,P) = 27.9$ Hz). The C_5H_4 signals were observed as multiplets at $\delta = 4.64$ and 4.70 ppm (**3a**) and at $\delta = 4.83$, 4.79, 4.64, and 4.57 ppm (**3b**). In the $^{31}P\{^1H\}$ NMR spectra, resonances for the P*i*Pr$_3$ and PCy$_3$ ligands appeared at $\delta = 47.1$ and 37.8 ppm, respectively. In the $^{13}C\{^1H\}$ NMR spectra, the signals for the C_{ipso} atoms were found at $\delta = 136.9$ (**3a**) and 138.1 ppm (**3b**). In the IR spectra, bands for the $\tilde{\nu}$(ReH) stretching vibrations were detected at 1976 (**3a**) and 1975 cm^{-1} (**3b**) and strong bands at 1629 (**3a**) and 1620 cm^{-1} (**3b**) were attributed to the $\tilde{\nu}$(NO) vibrations. The structures of compounds **3a** and **3b** were established by single-crystal X-ray diffraction, which showed quite similar bond-lengths and angles in the two structures. The structure of compound **3b** is shown in Figure 1 (for compound **3a**, see the Supporting Information). The half-sandwich complexes adopted a pseudo-tetrahedral geometry with planar η^5-$C_5H_4OSiMe_2tBu$ rings. The Re1−N1 bond lengths (1.749(5) (**3a**) and 1.740(3) Å (**3b**)) were within the expected range for rhenium–nitrosyl complexes (1.734–1.766 Å)[17] and the Re-N-O angles (178.4(6)° (**3a**) and 177.9(4)° (**3b**)) indicated linear NO-ligand binding in both cases. In contrast to the fact that only slight differences were seen in the bond-lengths of both compounds, significant deviations were observed between the angles, with a maximum difference of 7.2° for the N1-Re1-H angle (90(3)° (**3a**) and 97.2(19)° (**3b**)), which was presumably due to different Tolman cone-angles of P*i*Pr$_3$ (160°) and PCy$_3$ (170°).[18]

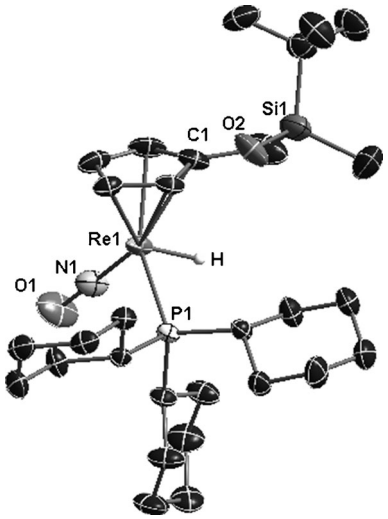

Figure 1. Molecular structure of compound **3b**. Thermal ellipsoids are set at 50% probability. All hydrogen atoms are omitted for clarity, except for the hydride atom. Selected bond lengths [Å] and angles [°]: Re1–H 1.63(6), Re1–N1 1.740(3), Re1–P1 2.3752(9), N1–O1 1.209(5), C5–O2 1.355(7); Re1-N1-O1 177.9(4), N1-Re1-P1 91.85(13), N1-Re1-H 97.2(19), P1-Re1-H 81(2).

[Re(H)(NO)(PR_3)(C_5H_4O)][NBu_4] (4a and 4b): Next, the anionic complexes [Re(H)(NO)(PR_3)(C_5H_4O)][NBu_4] (R = *i*Pr_3 (**4a**), Cy (**4b**)) were formed through deprotection of the siloxy group. Cleavage of the Si–O bond of the *tert*-butyldimethylsiloxy group with tetrabutylammonium fluoride (TBAF) afforded, after purification, the [Re(H)(NO)(PR_3)(C_5H_4O)][NBu_4] compounds in moderate to good yields (**4a**: 64%, **4b**: 85%). In the ^{1}H NMR spectra, the hydride signals shifted to lower field ($\delta = -8.01$ (**4a**), -8.11 ppm (**4b**)) with respect to the complexes of type **3**. In both cases, the H_{Cp} resonances appeared as four multiplets in the range $\delta = 5.56$–3.25 ppm. In the ^{31}P{^{1}H} NMR spectra, the signal of the P*i*Pr_3 ligand was observed at $\delta = 43.3$ ppm and the signal of the PCy_3 ligand was observed at $\delta = 31.7$ ppm. In comparison with the ^{13}C NMR chemical shift of the C_{ipso} carbon atom in compounds **3a** and **3b** ($\delta = 136.9$ and 138.1 ppm, respectively) and the shifts for the CO group of the cyclopentadienone moiety in compounds **10a** and **10b** ($\delta = 171.4$ and 170.6 ppm, respectively; see below), the corresponding signals of the C_{ipso} ring atoms were observed at $\delta = 167.5$ (**4a**) and 167.2 ppm (**4b**), which indicated a reduced CO double-bond character with significant delocalization of the negative charge over the cyclopentadienyl ring and the metal center. The IR spectra of compounds **4a** and **4b** showed strong $\tilde{\nu}$(NO) bands at low wavenumber (1533 cm^{-1}) in comparison with those of compounds **3a** and **3b** (1629 and 1620 cm^{-1}, respectively), presumably owing to strong back-bonding from the rhenium center to NO.

[Re(H)(NO)(PR_3)(C_5H_4OH)] (5a and 5b): The bifunctional complexes [Re(H)(NO)(PR_3)(C_5H_4OH)] (**5a** (R = *i*Pr_3), **5b** (R = Cy)) were obtained by acidification of compounds **4a** and **4b** with ammonium bromide followed by purification using column chromatography on silica gel at −30 °C under a nitrogen atmosphere (Scheme 1). Compounds **5a** and **5b** were obtained as yellow solids in 50% yield, which showed high sensitivity towards oxygen; both compounds were fully characterized by elemental analyses and by various spectroscopic methods. The ^{1}H NMR spectra in [D_8]THF exhibited broad singlets at $\delta = 8.03$ ppm (**5a**/**5b**) for the acidic proton. The H_{Re} resonances were observed as doublets ($\delta = -9.42$ ppm, ^2J(H,P) = 27.4 Hz for **5a** and $\delta = -9.48$ ppm, ^2J(H,P) = 27.4 Hz for **5b**). In the IR spectra, the characteristic $\tilde{\nu}$(NO) and $\tilde{\nu}$(OH) vibrations were found at 1607 and 3118 cm^{-1} for compound **5a** and at 1620 and 3144 cm^{-1} for compound **5b**. The structure of compound **5a** was confirmed by single-crystal X-ray diffraction. It crystallized as a hydrogen-bonded dimer (Figure 2) with an OH···Re interaction.

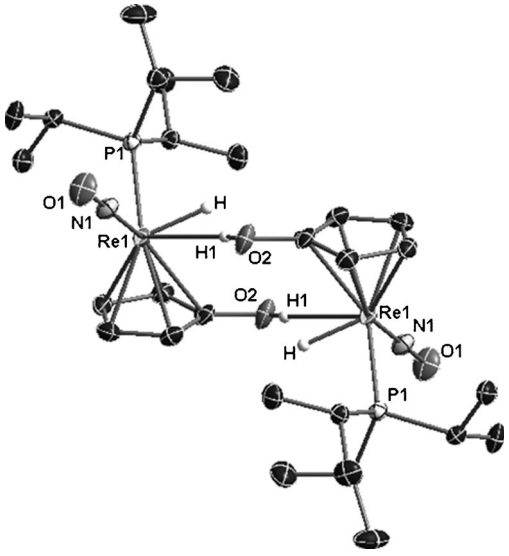

Figure 2. Molecular structure of the dimeric form of compound **5a**. Thermal ellipsoids are set at 50% probability. All hydrogen atoms are omitted for clarity, except for H and H1. Selected distances [Å] and angles [°]: Re1–H 1.57(4), Re1–N1 1.754(3), Re1–P1 2.397(10), N1–O1 1.212(4), Re1···H1 2.73(5), H···H1 2.03(6); Re1-N1-O1 179.5(3), N1-Re1-P1 91.33(11), N1-Re1-H 100.3(14), P1-Re1-H 76.5(14), O2-H1···Re1 169(4).

In the dimer, the acidic proton H1 pointed towards the other rhenium center, with a Re···H non-bonding distance of 2.73(5) Å. The distance between the acidic proton and the hydride atom was 2.03(6) Å, which was within the range of dihydrogen bonding.[19] The rhenium centers possessed pseudo-tetrahedral geometries and the η^5-C_5H_4OH rings on top of the metal were planar. The nitrosyl ligand was bound in an almost-linear geometry to the metal center (Re-N1-O1 179.5(3)°) and showed a N1-Re-H angle of 100.3(14)°, which was 10° wider than for compound **3a**.

NMR spectroscopy of the isomerization of compounds 5a and 5b in nonpolar solvents: NMR spectroscopy of compounds **5a** and **5b** revealed the presence of a second, structurally quite-different species, which preferentially appeared

in non-polar solvents (toluene, benzene, CH_2Cl_2). We attributed these signals to *trans*-dihydride cyclopentadienone complexes **6a** and **6b**, which were formed from compounds **5a** and **5b**, respectively, in equilibrium reactions (Scheme 2).

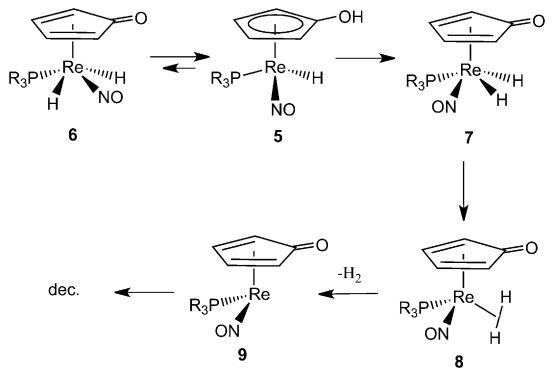

Scheme 2. Isomerization and decomposition pathway for compounds **5a** and **5b**.

Compounds **6a** and **6b** could not be isolated. The ^{1}H NMR spectra in [D$_8$]toluene showed signals for the cyclopentadienone ring that were split into two C*H* multiplets. The doublets at $\delta = -3.50$ ppm (^2J(H,P) = 47.3 Hz, **6a**) and $\delta = -3.18$ ppm (^2J(H,P) = 47.0 Hz, **6b**) were assigned to the two magnetically and chemically equivalent hydride ligands. This coupling pattern was in agreement with their *trans* position and a freely rotating or symmetrically bound C_5H_4O ring. In the ^{13}C{^{1}H} NMR spectra, the carbonyl signals of the cyclopentadienone rings appeared at $\delta = 175.0$ ppm for compound **6a** and at $\delta = 181.6$ ppm for compound **6b**. These signals were strongly upfield-shifted in comparison with those of compounds **4a** and **4b** ($\delta = 167.5$ (**4a**) and 167.2 ppm (**4b**)) and were slightly upfield of the corresponding signals in compounds **10a** and **10b** ($\delta = 171.4$ (**10a**) and 170.6 ppm (**10b**)). The T_1 relaxation times, as measured by the inversion-recovery method, of compounds **6a** and **6b** (562 and 317 ms, respectively) at 293 K confirmed the dihydride structure.[20] In the presence of *cis*-dihydride or dihydrogen complexes of type **7** or **8**, the ^{1}H NMR spectra would require the appearance of AB- or AX-type patterns for the hydride ligands in compounds **7a** and **7b** or a broad signal that was typical for the fast-rotating H_2 ligand in compounds **8a** and **8b**; however, such signals could not be detected. Furthermore, the IR spectra supported the presence of one new species, because only one new $\tilde{\nu}$(NO) band (at 1713 cm^{-1} for **6a** and at 1712 cm^{-1} for **6b**) was observed, both of which were shifted to higher wavenumber with respect to compounds **5a** and **5b**.

In non-coordinating solvents, compounds **5a** and **5b** decomposed at 60 °C, presumably owing to H_2 evolution from the activated cyclopentadienone–dihydrogen complex that was in equilibrium at this temperature (Scheme 2). However, a signal that corresponded to the H_2 moiety could not be traced with confidence in the spectra of the decomposed complexes, because, in the expected region ($\delta \approx 4.2$ ppm), the signals overlapped with those of the cyclopentadienone ligand or of the decomposition products. The structures of the molecules shown in Scheme 2 were calculated by using DFT (Figure 3 and Figure 5). The calculated energy for the dissociation of the H_2 ligand from complex **D** to form complex **E** (Figure 5) was 76 kJ mol^{-1}. Taking this value as a benchmark for the analogous reaction of compounds **5a** and **5b**, this result confirmed the thermal accessibility of H_2-liberation from these molecules at 60 °C. Furthermore, for compounds **5a** and **5b**, we anticipated that hydrogen bonding to hydrogen-bond acceptors, such as polar solvent molecules (DMSO, THF, MeCN, and 2-propanol), would stabilize the hydroxy cyclopentadienyl structure and enforce the thermodynamic preference for these isomers over the *trans*-dihydride structures. In [D$_8$]THF, as an exemplary more-polar solvent, the ^{1}H NMR spectra of compounds **5a** and **5b** revealed the presence of only hydroxy-cyclopentadienyl–monohydride–rhenium complexes in the temperature range −90–+60 °C.

1D NOE/EXSY of [Re(H)(NO)(PR$_3$)(C$_5$H$_4$OH)] (5a and 5b): The proton-exchange equilibria of complexes **5a** and **5b** via **6a** and **6b** were investigated by using 1D NOE/EXSY experiments in [D$_8$]THF and [D$_8$]toluene over the temperature range 20–60 °C. Irradiation of the H_{Re} signal did not lead to any response from the acidic OH proton at 22 °C, which was interpreted as no exchange between the H_{Re} and OH protons on the NMR timescale. This exchange-reaction became visible for compound **5a** at 42 °C, with the appearance of a negative H_O signal in [D$_8$]THF ($\delta =$ 8.15 ppm) and at 32 °C in [D$_8$]toluene ($\delta = 7.00$ ppm). In [D$_8$]toluene, an additional response was seen at 52 °C, with the enhancement of the *trans*-dihydride signal ($\delta =$ −3.05 ppm). The related proton-exchange reaction of compound **5b** was observed at 52 °C in MeCN, but not in [D$_8$]THF. In [D$_8$]toluene, the response signals became observable at temperatures 10 °C higher than for compound **5a**. The reversible OH proton-exchanges, which presumably occurred via the *trans*-dihydrides **6a** and **6b**, were also expected to lead to racemization at the rhenium centers of compounds **5a** and **5b**.

Reaction of compounds 5a and 5b with D$_2$O and D$_2$: Because the proton-exchange reactions described above were already noticeable in the range 40–50 °C, we also followed the H/D exchanges by using D_2O and D_2 at room temperature. The H_2-exchange reactions were anticipated not to proceed via *trans*-dihydrides **6a**/**6b**, but rather via an equilibrium between *cis*-dihydrides (**7**) and their related dihydrogen complexes (**8**; Scheme 2). H/D-exchange reactions with D_2 were studied in [D$_8$]THF under 1.5 bar D_2. ^{1}H NMR spectroscopy of the reactions of compounds **5a**/**5b** at room temperature showed a hydride signal that decreased in intensity over time. After 77 h, the exchange of the H_{Re} atom amounted to 85 % for compound **5a** and 55 % for compound **5b**, and the exchange of the H_O signal to 100 % for compound **5a** and 77 % for compound **5b**, which clearly in-

dicated ongoing H_2/D_2 exchange at room temperature that could not be derived from the 1D NOE/EXSY spectra. By applying excess D_2O, ^1H NMR spectroscopy showed 94% H/D exchange of the hydridic hydrogen atom for compound **5a** and 92% for compound **5b** within 5 h. In all cases, the acidic proton exchanged faster than the H_{Re} proton. For the deuterium exchange of compounds **5a/5b** with D_2, we anticipated that a *cis*-dihydride (**7**) compound was formed first (Scheme 2). H_2-loss was proposed to occur in these experiments through an η^2-H_2 structure (type **8**) to afford the $16e^-$ species of type **9**, which, for complete exchange, had to be reloaded with H_2 or D_2 (see the DFT calculations, Figure 3 and Figure 5). Furthermore, we monitored the exchange reaction of the H_{Re} hydride of compounds **3a** and **3b** in [D_8]2-propanol, as well as under 1.5 bar D_2 in [D_8]THF at room temperature by ^1H NMR spectroscopy. In both cases, the intensity of the hydride signal did not change over 48 h, thereby indicating that the [Re(H)(NO)(PR_3)($C_5H_4OSiMe_2tBu$)] complexes were not susceptible to exchange, because, for these compounds, no pathway existed to form H_2 complexes. The Shvo-type ruthenium–hydride complex [({2,5-Ph_2-3,4-Tol_2(η^5-C_4CO)H})Ru($CO)_2$(μ-H)] was found to display faster exchange and, in either case, hydrogen-atom-selective RuH/RuD exchange with D_2 (4 atm); moreover, the exchange of the C_5H_4OH proton exclusively occurred in D_2O.[21] A related iron system reported by Casey and Guan[7c] showed 18% exchange of both types of hydrogen atoms within 27 h, thus indicating much-lower activity in these H-exchange reactions than compounds **5a/5b**.

DFT study of the equilibrium between tautomers 5a/5b and 6a/6b: The formation of the *trans*-dihydrides of type **6** was further studied by DFT calculations on freely optimized PMe_3-substituted model compounds (**A**–**E**) and on the transition states (**TS1**–**TS5**) by using the B3LYP[22] functional and the 6-31G (d,p)[23] basis set for H-P and the LANL2DZ[24] basis set in connection with the associated effective core potential for Re with the GAMESS program package.[25] All free energies were calculated at 298.15 K and referenced to the energy of structure $\mathbf{A_1}$.

Three stable rotational isomers were found for tautomer **A**, with $\mathbf{A_1}$ as the local minimum. In all of these cases, the C_{ipso} atom of the hydroxy cyclopentadienyl ring (C_5H_4OH) possessed the longest Re–C bond. In the local minima, the C_{ipso} atom eclipsed one of the tripod axes (Re–H 0.0 kJ mol^{-1}, $\mathbf{A_1}$; Re–PMe_3 0.1 kJ mol^{-1}, $\mathbf{A_2}$; or Re–NO 8.9 kJ mol^{-1}, $\mathbf{A_3}$; Figure 3). The long Re–C_{ipso} bond was interpreted in terms of an early outline of an incipient butadiene character in the Re–C bonds that was not yet reflected in the C–C bond lengths of the C_5H_4OH ring. Because the NMR spectra suggested a free rotation of the C_5H_4OH ring in compounds **5a/5b**, we assumed that rotamers $\mathbf{A_1}$–$\mathbf{A_3}$ (energy span of less than 9 kJ mol^{-1}) were populated according to the relative energies of the $\mathbf{A_1}$, $\mathbf{A_2}$, and $\mathbf{A_3}$ models, with an equilibrium ratio of 1:0.95:0.3. In rotamer $\mathbf{A_1}$, the hydride and the proton were in a favorable arrangement for concerted bifunctional H_2-transfers in the secondary coordination sphere (H···H distance 3.06 Å). For the *trans*-H dihydride complex (**B**), three stable rotamers were calculated as the local minima on the energy hypersurface. As in the case of the rotamers of type **A**, the C=O bond of either structure of the cyclopentadienone conformers was eclipsed by either the Re–H (2.7 kJ mol^{-1}, $\mathbf{B_1}$), Re–P (5.4 kJ mol^{-1}, $\mathbf{B_2}$), or the Re–NO bond (24.4 kJ mol^{-1}, $\mathbf{B_3}$). The gas-phase free energies of the most-favored *trans*-H dihydride structure ($\mathbf{B_1}$, 2.7 kJ mol^{-1}) was close to the energy of the ground-state structure ($\mathbf{A_1}$, 0.0 kJ mol^{-1}). By qualitatively including the potential for hydrogen bonding to the **A** and **B** PMe_3 model structures, we estimated that structure $\mathbf{A_1}$ would be the preferred isomer in polar solvents, whilst structure $\mathbf{B_1}$ would be more favored in non-polar solvents, which reflected the experimental equilibrium positions quite well. In the case of the *cis*-dihydride species (**C**), three stable rotamers were optimized as local minima. For which the C=O bond was either eclipsed by the Re–H ($\mathbf{C_1}$, 20.1 kJ mol^{-1}), the Re–P ($\mathbf{C_2}$, −20.2 kJ mol^{-1}), or by the Re–NO bond ($\mathbf{C_3}$, 29.1 kJ mol^{-1}) for the same reasons as for the **A** and **B** structures. In addition, in comparison with the **A** and **B** isomers, the cyclopentadienone ring showed a pronounced butadiene structure with a "leg in the hole" conformational preference for the *cis*-diene.[26] The free-energy span for these **C**-type rotamers was larger, with the most-favorable conformer ($\mathbf{C_2}$) at lower energy than conformers $\mathbf{A_1}$ or $\mathbf{B_1}$. Next, the dihydrogen complex (**D**), which was related to the *cis*-dihydride structures of type $\mathbf{C_1}$, was structurally optimized, thereby revealing only the $\mathbf{D_1}$ conformer to be a local energetic minimum

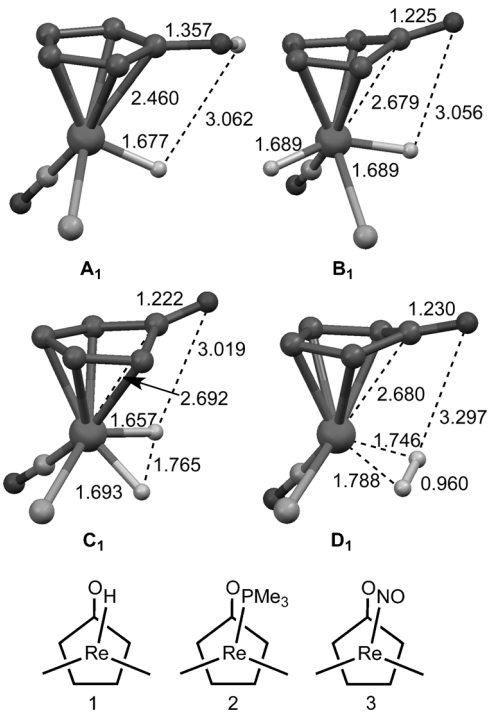

Figure 3. The lowest-energy rotamers of complexes **A**–**D** and selected bond lengths [Å]. The methyl groups of the PMe_3 ligands and the protons of the C_5H_4 rings are omitted.

(Figure 3). Conformer $\mathbf{D_1}$ was energetically less-favored than conformer $\mathbf{A_1}$ by 43.0 kJ mol^{-1} and by 20.1 kJ mol^{-1} relative to the *cis*-dihydride structure ($\mathbf{C_1}$). Although conformers $\mathbf{C_1}$ and $\mathbf{D_1}$ were structurally very similar, they were connected by a transition state (**TS5**) at relatively high energy: 78.0 kJ mol^{-1} above conformer $\mathbf{C_2}$, 35.0 kJ mol^{-1} above conformer $\mathbf{D_1}$, and 57.9 kJ mol^{-1} above conformer $\mathbf{C_1}$. Releasing H_2 from conformer $\mathbf{D_1}$ to form the unsaturated 16e$^-$ cyclopentadienone complex [Re(NO)(PMe$_3$)(C$_5$H$_4$O)] (**E**, 119.0 kJ mol^{-1} with respect to $\mathbf{C_2}$) revealed that the H_2 ligand was strongly bound to the Re center in conformer $\mathbf{D_1}$ (dissociation energy $D(H_2)=76.0$ kJ mol^{-1}). Overall, these DFT-calculated energies suggested that, in solutions of compounds **5a/5b**, a *cis*-dihydride structure that was analogous to conformer $\mathbf{C_2}$ was the main constituent. However, this result was, to some extent, in contrast to the experimental data; therefore, we tried to further analyze the kinetic results. A reaction path that connected the **A** and **C**-type structures seemed to be inaccessible under ambient conditions. To find a kinetically meaningful mechanism for the equilibrium between compounds **5a/5b** and **6a/6b**, excluding formation of the *cis*-dihydrides, we optimized all of the possible transition states for the interconversion between complexes **A**–**D**. In the first step, the transition states of the direct transfer of the H_O proton to the metal center and its reverse were calculated. However, the transition states that connected complex $\mathbf{A_1}$ with $\mathbf{B_1}$ (**TS1**, 174.4 kJ mol^{-1}; see Figure 4) and complex $\mathbf{A_1}$ with $\mathbf{D_1}$ (**TS2**, 156.0 kJ mol^{-1}), through proton transfers to the rhenium and H_{Re} atoms, respectively, were found at high energies; hence, they were not considered to be operative in the exchange processes.

Proton transfer from the H_O atom to the rhenium center in transition state **TS1** proceeded via a strained four-membered ring, whilst proton transfer to the H_{Re} atom via **TS2** proceeded via a five-membered ring in a less-strained geometry. This latter process resembled the frequently observed protonation of hydride complexes, which almost exclusively occurs in a kinetically controlled fashion at the hydride site.[27] An additional observation was that the proton-transfer in **TS1** was accompanied by a short Re–C$_{ipso}$ bond (2.319 Å), which was much-shorter than the same process via **TS2** (2.427 Å) and also shorter than in the **A**-type structures (2.418 Å). Moreover the O_{CO} atom was bent towards the Re center (**TS1**: 11.5°, **TS2**: 14.7°). This bending was anticipated to impose strain on these structures and to be supported by an "inserted" hydrogen-bonding auxiliary that mediated the H^+ transfer. Ito and Ikarya attributed similar auxiliary functions to acidic HX groups in bifunctional ruthenium catalysts,[28] which enabled the acceleration of transfer-hydrogenation reactions owing to the role of hydrogen-bonding reagents in organocatalysis.[29] Therefore, we calculated transition states that included a water molecule as potential proton donor or -acceptor. The calculations revealed the existence of a **TS3**···H_2O state at an energy of 96.2 kJ mol^{-1} relative to an $\mathbf{A_1}$···H_2O "hydrate", thereby enabling connection of the *trans*-hydride $\mathbf{B_1}$···H_2O with $\mathbf{A_1}$···H_2O. Although the hydrogen-bonded structure $\mathbf{C_1}$···H_2O, which was relevant for the H_O proton-transfer to the rhenium center, could be traced as a local minimum in which a single H_2O molecule bridged the C$_5$H$_4$OH group and the rhenium center of $\mathbf{A_1}$, no transition state was found for the transition of $\mathbf{A_1}$···H_2O into $\mathbf{C_1}$···H_2O. An alternative pathway from **A**-type to **C**-type structures was imagined to proceed via the initial formation of structure **B**, which was then transformed into **C**. Therefore transition state **TS4** was optimized, in which one of the hydrides of structure $\mathbf{B_1}$ was pushed toward the PMe$_3$-Re-NO plane. Transition state **TS4** (144.4 kJ mol^{-1}) was 11.6 kJ mol^{-1} more favorable in free energy than **TS2**. The computational results agreed with the existence of pathways for the equilibrium between compounds **5a/5b** and **6a/6b**. Mechanistic paths that proceeded via the dissociation of the PMe$_3$ ligand or via ring-slippage were also tested but were excluded owing to the high binding energy of the PMe$_3$ ligand in structure **A** (198.5 kJ mol^{-1}) and the inability to find local energetic minima for an unsaturated η^3-haptotropic [ReH(η^3-C$_5$H$_4$OH)(NO)(PMe$_3$)] species. Furthermore, although dihydride structure $\mathbf{C_2}$ would be preferred over **A** and **B**, a high kinetic barrier strictly separated this isomer from the **A**⇌**B** equilibrium. This result had two important consequences for the reactivity of the system (Figure 5): 1) The hydrogen release/addition equilibrium **A**⇌**E**+H_2 (**E**=[Re(NO)(PMe$_3$)(η^4-cyclopentadione)]) was hampered by high kinetic barriers, which were even higher than the H_2-affinity of **E** (119.0 kJ mol^{-1}). 2) The regeneration of structure **A** from **E** with H_2 was envisaged to proceed via a **C**-type species, but this was also not a facile process, with a relatively high energetic barrier for the conversion of a dihydride into structures **A** or **B**. These findings made it clear that hydrogenation reactions with catalysts **5a/5b** would be associated with relatively harsh conditions.

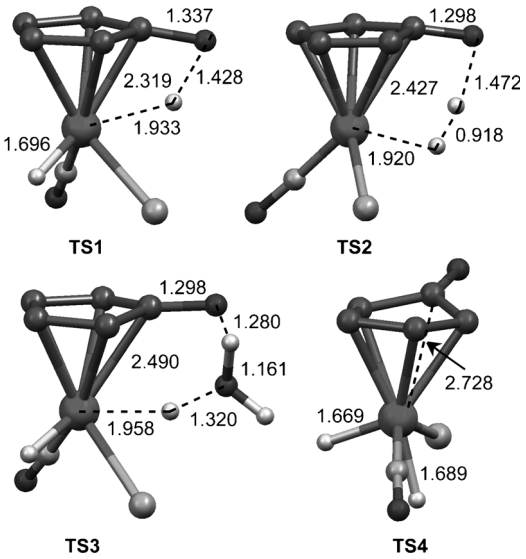

Figure 4. Transition states **TS1**–**TS4** and selected bond lengths [Å]. PMe$_3$ methyl groups and protons of the Cp rings are omitted.

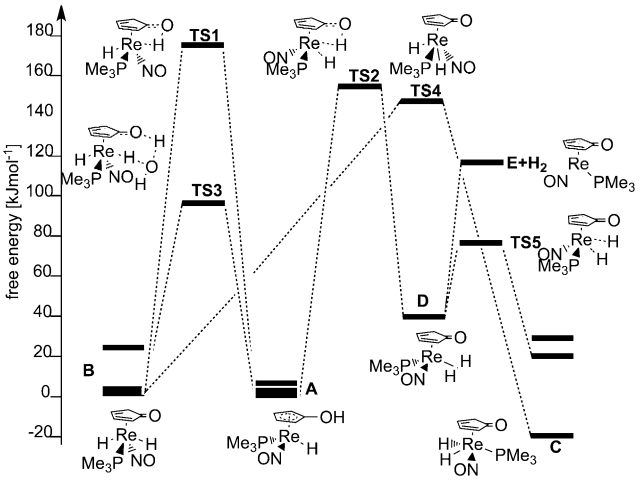

Figure 5. Free-energy diagram [kJ mol^{-1}] of compounds **A**–**E** and their connecting transition states **TS1**–**TS5** at 298.15 K.

Catalytic activity of compounds 5a and 5b in the transfer-hydrogenation reactions of ketones and imines: We explored the catalytic potential of compounds **5a** and **5b** in the transfer-hydrogenation reactions of various ketones and imines with 2-propanol as both a solvent and a hydrogen donor. The comparably low hydrogenation enthalpy of acetone (-69.7 kJ mol^{-1})[30] made 2-propanol a versatile reactant in such reactions. The **5a/5b**⇌**6a/6b** tautomerization was another reason to choose a polar solvent, because it was expected to favor higher effective concentrations of the catalyst (**5a/5b**). In addition, it seemed appropriate to stabilize the highly activated intermediates **9a** and **9b** through hydrogen-bonding interactions with 2-propanol (see below).

The addition of 0.5 mol% of compound **5a/5b** efficiently catalyzed the reduction of ketones and imines in 2-propanol (30 equiv with respect to the substrates) at 120°C (Table 1). For example, we obtained the highest TOF for acetophenone by using catalyst **5a** (TOF = 1164 h^{-1}, 97% conversion after 10 min), as determined by GCMS. Aryl ketones were hydrogenated more-rapidly than, for instance, the alkyl ketone pinacoline (Table 1, entry 5). The nonpolar olefin double bond (Table 1, entry 8) was not hydrogenated by catalysts **5a/5b** and ketones were hydrogenated much faster than imines (Table 1, entries 9–11). Except for the transfer-hydrogenation reactions of acetophenone and *p*-diacetylbenzene, the catalytic performances of compounds **5a** and **5b** were comparable.

Imines were reduced more-efficiently with compound **5b** than with compound **5a**. To confirm that the combination of the hydridic H_{Re} and the acidic H_O atoms was required for catalytic activity, we tested compounds **3a** and **3b**, which only contained the hydridic functionality. Using 1.2 mol% of compound **3a** or **3b**, the transfer-hydrogenation reaction of acetophenone in [D_8]2-propanol was monitored at 80°C by using ^{1}H NMR spectroscopy. After 24 h, we detected 21.2% (**3a**, TOF = 0.7 h^{-1}) and 2.5% (**3b**, TOF = 0.1 h^{-1}) reduction of acetophenone, which indicated a much-lower catalytic activity compared to compounds **5a** and **5b**. These very low activities were attributed to the presence of traces of compounds **5a** and **5b** that were generated by silyl deprotection of compounds **3a** and **3b**, either owing to the presence of traces of water or to an as-yet-unknown reaction pathway.

Table 1. Transfer hydrogenation of ketones and imines catalyzed by [Re(H)(NO)(PR_3)(C_5H_4OH)] (**5a** and **5b**).[a]

Entry	Substrate	Catalyst	*t*	Yield [%][b]	TOF [h^{-1}]
1	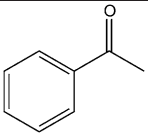	**5a**	10 min	97	1164
		5b	30 min	95	380
2	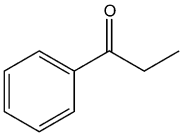	**5a**	1.5 h	98	131
		5b	1.5 h	96	128
3	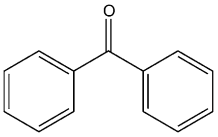	**5a**	45 min	98	261
		5b	45 min	99	264
4	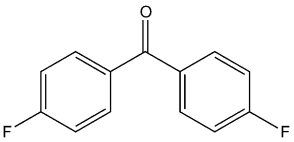	**5a**	1 h	98	196
		5b	3 h	98	65
5	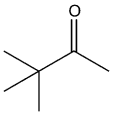	**5a**	2.5 h	97	78
		5b	2.5 h	92	74
6	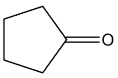	**5a**	1 h	98	196
		5b	35 min	94	322
7	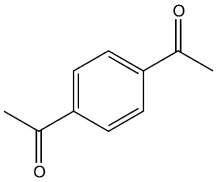	**5a**	2 h	81[c]	81
		5b	2 h	0	0
8	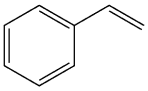	**5a**	1.5 h	0	0
		5b	1.5 h	0	0
9	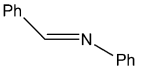	**5a**	3 h	97	65
		5b	2.5 h	99	79
10	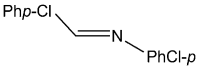	**5a**	3 h	73	49
		5b	3 h	86	57
11	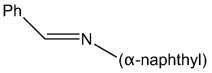	**5a**	5 h	77	31
		5b	5 h	90	36

[a] Conditions: substrate (0.436 mmol), catalyst (**5a/5b**; 0.00218 mmol, 0.5 mol%), 2-propanol (1 mL), 120°C. [b] Yield determined by GCMS analysis. [c] 19% mono-hydrogenated product obtained.

Transfer hydrogenation of benzaldehyde: The reductions of benzaldehyde with compounds **5a/5b** (1 mol%) in [D_8]2-propanol at 350 K were monitored by ^{1}H NMR spectrosco-

py. Quite unexpectedly, these reactions were found to be slow. After 4 h, 75% (**5a**, TOF = 19 h^{-1}) and 72% conversion (**5b**, TOF = 18 h^{-1}) of the aldehyde were observed, much lower than the analogous reductions of acetophenone after 30 min in the presence of 1.2 mol% of compounds **5a**/**5b** (**5a**: 80%, TOF = 133 h^{-1}; **5b**: 90%, TOF = 151 h^{-1}). Moreover, the reaction solution became green during the catalysis and the typical signal for the catalyst in the ^{31}P NMR spectra disappeared, with the concomitant formation of various unidentified signals. Presumably, the formed benzyl alcohol reacted with the catalyst, thus blocking the catalytic system. To confirm this idea, we monitored the reduction of acetophenone in [D_8]2-propanol in the present of excess benzyl alcohol at 77°C by ^{31}P NMR spectroscopy. After 30 min, two new signals appeared at $\delta = 22.8$ ppm (12%) and $\delta = 24.3$ ppm (13%), which were not detected in reactions without benzyl alcohol. Changing the solvent and hydrogen donor from [D_8]2-propanol to [D_4]MeOH in the reduction of acetophenone, the ^1H NMR spectra indicated about 43% conversion (TOF = 3.9 h^{-1}) after 22 h at 77°C. In addition, the ^{31}P NMR spectra indicated a decrease in the catalyst signal and the appearance of new unidentified signals. The solution also turned green, as in the reaction of benzaldehyde. From this result, we concluded that primary alcohols could react with active species **5a**/**5b**, or even, most likely, with 16e^- intermediates of type **9**. Related investigations on the formation of alcohol complexes were carried out by Casey and Guan by using the iron complex [{2,5-($SiMe_3$)$_2$-3,4-$(CH_2)_4$(η^5-C_4COH)}Fe$(CO)_2$(H)] as a transfer-hydrogenation catalyst. Indeed, iron–alcohol complexes were observed in toluene in the present of equivalent amounts of benzaldehyde, and were stable at −30°C, but underwent decomposition within 1 h at room temperature.[7c] DFT calculations reported by Chen et al. described these alcohol complexes as the most-stable species in the cycle.[7a]

The effect of water in the transfer-hydrogenation reactions: It has been reported that water had an influence on the catalytic performance of Shvo-type ruthenium complexes in transfer-hydrogenation reactions; however, these effects were difficult to rationalize on the basis of a mechanistic scheme.[3a,4a] Therefore, we wanted to test the influence of water in rhenium-based systems, and chose the transfer-hydrogenation reactions of acetophenone catalyzed by compounds **5a**/**5b** in [D_8]2-propanol in the presence of various amounts of water. The reactions were monitored by ^1H NMR spectroscopy. Catalyst **5a** (1.2 mol%) showed a decrease in catalytic activity with increasing amounts of water: After 5 min, 27% (0 equiv), 23% (40 equiv), and 20% (80 equiv) reduction of acetophenone were observed at 350 K. However, in the presence of compound **5b** (1.2 mol%), an increase in the catalytic activity was observed with the addition of up to 40 equiv H_2O relative to the catalyst, but more water led to a decrease in activity. After 5 min, 39% (0 equiv), 72% (40 equiv), and 25% (80 equiv) conversion into 1-phenylethanol was detected. With longer reaction times, the differences between the conversions of acetophenone became approximated. We envisaged two ways in which water could interact with the catalysts to have the observed effects on the rate of transfer-hydrogenation (Scheme 3): 1) water might stabilize and activate the substrate during the transfer-hydrogenation reaction, thereby leading to an increase in the catalytic activity, or 2) water could inhibit the catalysis by forming hydrogen-bonding interactions with the acidic proton and the hydridic hydrogen atom of compounds **5a**/**5b**, or fully coordinate to the rhenium center of unsaturated species **9**, thereby forming catalytically inactive or less-active water complexes [Re(C_5H_4O)(NO)(OH_2)(PR_3)]. To find out whether hydrogen bonding or direct interaction to the Re center with water caused the decrease in catalytic activity, we monitored related experiments by ^1H NMR spectroscopy by using the strong hydrogen-bond-donor hexafluoro-2-propanol. After 30 min at 350 K, we observed a steady decrease in the catalytic activity, with 81% (0 equiv), 77% (20 equiv), 39% (40 equiv), and 22% (60 equiv) conversion for compound **5a**. The same trend was observed for compound **5b**, with 90% (0 equiv), 77% (20 equiv), 42% (40 equiv), and 24% (60 equiv) in the reduction of acetophenone. These observations supported the idea of a decrease in the catalytic activity in presence of strong hydrogen-bond donors.

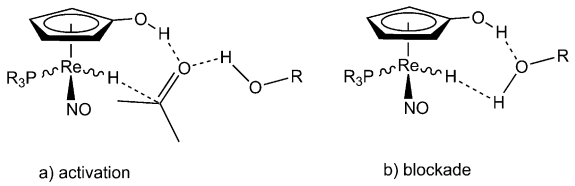

Scheme 3. Possible modes of HOR interaction with compounds **5a** and **5b**.

DFT modeling of the transfer hydrogenation of ketones with [Re(H)(NO)(PMe_3)(C_5H_4OH)] (A): With regards to Shvo's catalyst,[7d] primary- and secondary-coordination-sphere mechanisms were envisaged to be operative in the transfer-hydrogenation reactions with compounds **5a**/**5b**. Therefore, we modeled these processes by using DFT calculations with the PMe_3 analogues of type **A** as starting points. H_2CO and CH_3CHO were selected as substrates because their gas-phase hydrogenation enthalpies ($\Delta H_{hydr.} = -92.4$ and −68.6 kJ mol^{-1}, respectively[30]) were thought to be representative of a wide range of carbonyl compounds. Key to an efficient primary-coordination-sphere mechanism would be the binding of the substrate to the Re center. Because compound **A** was an 18e^- complex, this binding would require either 1) the replacement of the phosphine ligand, 2) a hapticity change of the C_5H_4OH ligand, or 3) bending of the NO ligand. Substitution of the PMe_3 ligand following a dissociative mechanism would proceed through the generation of the [ReH(η^5-C_5H_4OH)(NO)] intermediate, which was 198.5 kJ mol^{-1} higher in free energy than compound **A**. Under real catalytic conditions with compound **5a**/**5b**, either

at room temperature or at 100 °C, this barrier would be insurmountable. However, an interchange mechanism in which the PMe_3 ligand was replaced directly, could lower the barrier to access $[ReH(CH_2O)(\eta^5\text{-}C_5H_4OH)(NO)]$ to 93.0 kJ mol^{-1}, which marked the lower limit of the thermodynamics of this process.

However, this activation barrier would still be too high compared to a secondary-coordination-sphere mechanism, in which hydrogen-bonding interactions are the decisive substrate interactions (see below). The creation of a free coordination site via ring-slippage or NO-bending would lead to the formation of $[ReH(CH_2O)(\eta^3\text{-}C_5H_4OH)(\text{linear-NO})(PMe_3)]$ or $[ReH(CH_2O)(\eta^5\text{-}C_5H_4OH)(\text{bent-NO})(PMe_3)]$ intermediates. However, no such structures were traced as local minima on the potential-energy hypersurface for the CH_2O complexes. This result was interpreted in terms of the formation of a too-weak $Re{-}O_{(CO)}$ bond with the aldehyde, which could not compensate for the breakage of the stronger $Re{-}C_{(C_5H_4OH)}$ bond or the bending of the nitrosyl group. In this respect, the Re–NO system differed from the analogous Ru–CO systems,[7d] for which an associative primary-coordination-sphere mechanism that involved ring-slippage could be made plausible by DFT calculations.[7d]

Thus, the secondary-coordination-sphere mechanism was investigated as an alternative, for which the geometries of the crucial species were optimized without constraints (Figure 6). The calculated free energies (Figure 7) revealed a low-energy reaction path that would be accessible under real catalytic conditions if transposed to the transfer hydrogenation reactions with compounds **5a**/**5b**. Next, we focused on the transfer-hydrogenation reaction of the CH_2O/CH_3OH couple, because the transfer-hydrogenation reaction of the CH_3CHO/CH_2CH_2OH couple was calculated to be very similar in terms of the geometric parameters of the structures. Starting from structure **A**, the first step was the formation of a hydrogen bond between the substrate and

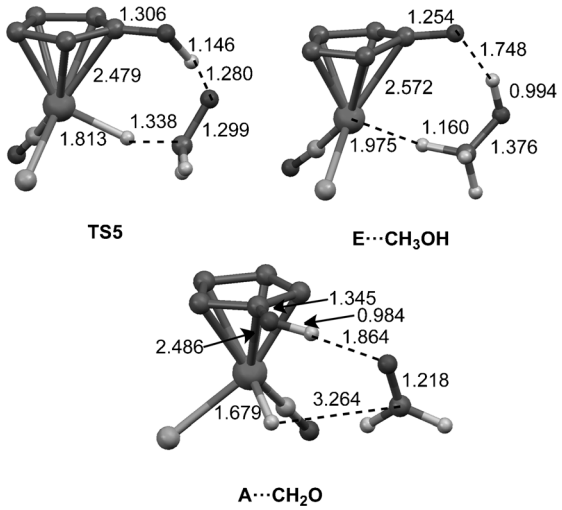

Figure 6. Drawings of transition state **TS5** and adducts **E···CH$_3$OH** and **A···CH$_2$O** with selected bond lengths [Å]. The PMe_3 methyl groups and the protons on the C_5H_4OH/C_5H_4O rings are omitted.

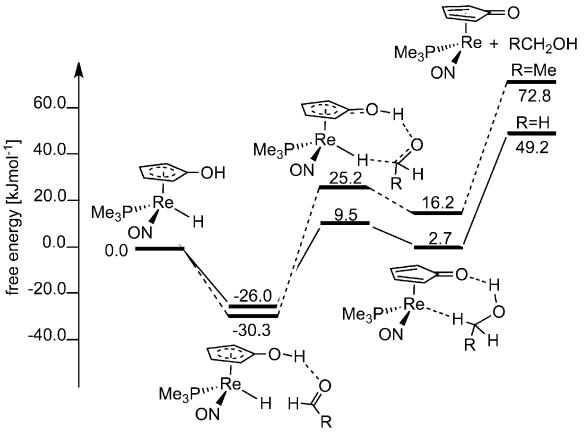

Figure 7. DFT-calculated free-energy diagram [kJ mol^{-1}] of the secondary-coordination-sphere double-H-transfer reaction at 298.15 K, starting from $[Re(H)(NO)(PMe_3)(C_5H_4OH)]$ (**A**), formaldehyde, and acetaldehyde to yield $[Re(C_5H_4OH)(NO)(PMe_3)]$ species **E** and MeOH or EtOH.

the C_5H_4OH hydroxy group, which was accompanied by a stabilization of −26.0 kJ mol^{-1} for the **A**···CH_2O arrangement. At this stage, the interaction between the $C_{(CO)}$ and the Re–H atom was negligible (Re–H···*C*H_2O 3.264 Å). In the next step, a concerted double-H-transfer was anticipated to occur from structure **A** to CH_2O via the seven-membered transition state **TS5** (9.5 kJ mol^{-1}), which was 35.5 kJ mol^{-1} higher in free energy than the **A**···CH_2O adduct. In transition state **TS5**, the bond between the Re–H and the CH_2O units was manifested in the shortening of the Re–H···*C*H_2O distance to 1.338 Å. At the same time, the C=O bond-length in CH_2O became stretched to 1.299 Å, which was intermediate in length between the C–O bond in **E**···CH_3OH (1.376 Å) and the C=O bond in **A**···CH_2O (1.218 Å). Likewise, the C_5H_4OH bond-length in transition state **TS5** (1.306 Å) lay structurally in between those in **A**···CH_2O (1.345 Å) and **E**···CH_3OH (1.254 Å), and the Re–H distance in transition state **TS5** (1.813 Å) lay in the middle of those in **A**···CH_2O (1.679 Å) and **E**···CH_3OH (1.975 Å). Therefore, we concluded that, in transition state **TS5**, the hydride group was shared equally between the Re-complex and the CH_2O substrate. At the same time, the C_5H_4OH proton still appeared to remain on the Re complex, as reflected by a relatively short C_5H_4O–H distance (1.146 Å) and a longer, but in absolute terms still quite short, C_5H_4OH···OCH_2 hydrogen-bonding distance (1.280 Å) when compared to **E**···CH_3OH (C_5H_4O···H 1.748 Å, H–OCH_3 0.984 Å). Thus, the proton transfer seemed to lag somewhat behind the hydride-transfer. Moreover the Re–C1 bond (2.479 Å) in transition state **TS5** was relatively short compared to the expected 2.529 Å (average of **A**···CH_2O and **E**···CH_3OH). Seemingly, the geometric requirements for the double-H-transfer outweighed the compression of the Re–C1 bond in transition state **TS5**. In a real system, we could imagine a more-concerted pathway that would involve protic functionalities that would be capable of relieving some of this strain. Following transition state **TS5**, **E**···CH_3OH was observed next

(+2.7 kJ mol^{-1}), which was 23.3 kJ mol^{-1} higher in free energy than **A**···CH_2O. Consequently, the **A**···CH_2O⇌**E**···CH_3OH equilibrium lay towards the left side, with only 0.008% of **E**···CH_3OH present at 298.15 K. In this structure, methanol was bound through a hydrogen bond to the cyclopentadienone ligand (C_5H_4O···$HOCH_3$ 1.748 Å) and through an agostic interaction between the Re center and a $H_{(Me)}$ atom (Re···HCH_2OH 1.975 Å). To complete the catalytic cycle, the formaldehyde in **A**···CH_2O and the methanol group in **E**···CH_3OH needed to be exchanged. The expected barrier for the carbonyl-exchange in **A**···CH_2O would be associated with the disruption of the H-bond, which amounted to a stabilization of −26.0 kJ mol^{-1}, thereby indicating a much-faster process than the concerted double-H-transfer (Figure 6). In contrast to this process, the exchange of the alcohol molecule in **E**···CH_3OH would formally require the splitting of the hydrogen bond and of the agostic interaction via the formation of structure **E** and free MeOH (46.5 kJ mol^{-1}), thereby leading to a free-energy span[31] of 75.2 kJ mol^{-1} in the gas phase. However, this energy only set an upper energy limit for the overall process, because it was more likely that this ligand exchange would proceed via several steps, each with lower barriers, and without the formation of the completely unsupported structure **E**. Such processes were difficult to model, because the involvement of solvent molecules might considerably stabilize the intermediates. For instance, a complex network of H-bonds and agostic interactions between the Re center and the P*i*Pr$_3$ or PCy_3 ligands could be envisaged. Therefore, we can safely state that the second coordination-sphere pathway was kinetically much-more favorable than any inner-coordination-sphere alternative. However, the overall free-energy barrier for this process is still to be considered a best guess, because the exchange of the alcohol in **E**···CH_3OH is also difficult to model with the methodology used.

In addition, we also modeled the H_2-transfer from structure **A** to acetaldehyde by using the secondary-coordination-sphere approach. Structurally, species **A**···MeCHO, **TS5**···EtOH, and **E**···EtOH resembled species **A**···CH_2O, **TS5**···MeOH, and **E**···CH_3OH, respectively, and the differences in the bond-lengths were usually less than 1%, with a few exceptions of up to 3%. However, energetically, the acetaldehyde cycle differed significantly from the formaldehyde cycle (Figure 7), mainly owing to the lower hydrogenation enthalpy of acetaldehyde (68.6 kJ mol^{-1}) compared to formaldehyde (92.4 kJ mol^{-1}).[30] This result demonstrated the often-observed close relationship between thermodynamics and kinetics. The two states, **A**···RCHO and **E**+RCH_2OH, defined the kinetics (or rather, they define an upper limit for the real free-energy span, see above). The energies of species **A**···RCHO and **E**+RCH_2OH could roughly be divided into energetic contributions from structures **A** and **E**, which were identical for both systems, and from the aldehydes and to the alcohols, which varied with their respective hydrogenation enthalpies, thereby establishing a tight connection between the thermodynamics and kinetics of the transfer-hydrogenation processes.

Trapping the cyclopentadienone intermediate: To acquire further support for the catalytic cycle, which we proposed to a large extent on the basis of DFT calculations, we tried to trap the spectroscopically untraceable 16e^- intermediates **9a**/**9b**. Therefore, the transfer-hydrogenation reaction of solutions of compounds **5a**/**5b** in 2-propanol and an excess of 2-butanone at 80 °C was quenched by the addition of pyridine. Overnight, complete conversion of compounds **5a**/**5b** into pyridine complexes **10a**/**10b** was observed (Scheme 4).

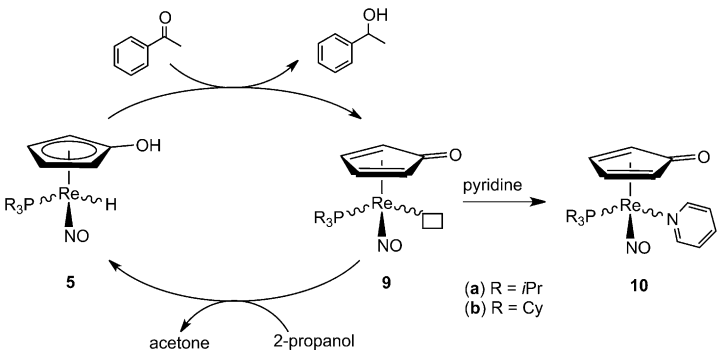

Scheme 4. Catalytic cycle for the reduction of acetophenone with compounds **5a** and **5b** and trapping of intermediate **9** with pyridine to obtain compounds **10a** and **10b**.

However, without the presence of either 2-butanone, pyridine, or changing the solvent from 2-propanol to THF, complexes **10a**/**10b** could not be obtained. We concluded that the transfer of H_2 from the hydrogen donor to an acceptor molecule was kinetically feasible, if potential ligands were available to stabilize the [Re(NO)(PR_3)(η^4-cyclopentadione)] fragment. The fact that 2-propanol could not be replaced by THF indicated that the 2-propanol complex of whatever structure was more stable than that with THF. Applying only pyridine without the presence of the 2-butanone to a solution of compounds **5a**/**5b** in 2-propanol at 80 °C resulted in conversion into compounds **10a**/**10b** in less than 10% yield after 15 h, which was in contrast to the full conversion of compounds **5a**/**5b** into compounds **10a**/**10b** in the presence of the H_2-acceptor 2-butanone. Thus, the Re system behaved markedly differently from the analogous Ru and Fe systems. In these cases, catalytic as well as stoichiometric H_2 transfers to acceptor substrates occurred concomitantly with dimerization to the bridged [Ru] dimers[21] or with PPh_3- and pyridine-trapped intermediates.[4a,5d]

The pyridine–cyclopentadienone complexes [Re(NO)(PR_3)(C_5H_4O)(py)] (**10a** (R = *i*Pr), **10b** (R = Cy)) were suggested to be formed according to Scheme 4. These species were fully characterized by NMR and IR spectroscopy, MS, and elemental analysis. The ^{1}H NMR spectra in [D_3]acetonitrile exhibited signals that corresponded to the C_5H_4O ligand: multiplets at δ = 6.07, 4.47, 4.26, and 3.26 ppm for compound **10a** and at δ = 6.00, 4.30, 4.22, and 3.23 ppm for compound **10b**. The C_{ipso} atoms were observed at δ = 171.4 ppm (**10a**) and at δ = 170.6 ppm (**10b**), which

were comparable to cyclopentadienone–dihydride complexes **6a** ($\delta = 175.0$ ppm) and **6b** ($\delta = 181.6$ ppm). In the ^{31}P NMR spectra, the signals of the phosphorus ligands shifted to higher field, from $\delta = 47.8$ ppm (**5a**) to $\delta = 21.8$ ppm (**10a**) and from $\delta = 36.5$ ppm (**5b**) to $\delta = 12.6$ ppm (**10b**). The structure of compound **10b** was established by single-crystal X-ray diffraction, which showed a non-planar C_5H_4O moiety (Figure 8). The C1 atom was located above the C2-C3-C4-C5 plane and the Re–C1 bond length was elongated (2.5678(16) Å). The former O2–C1 single bond in compound **5a** was converted into a double bond, with a distance of 1.249(2) Å. The exchange of the hydride ligand in the type-**3** structures for a pyridine ligand led to a widening of the angle to the PCy_3 ligand from 81(2)° (**3b**) to 93.14(4)° and the angle to the nitrosyl ligand from 97.2(19)° (**3b**) to 101.52(6)°, with a Re1–N2 bond length of 2.1540(14) Å. The isolated complexes (**10a**/**10b**) were stable in 2-propanol at room temperature; however, on heating to 80 °C for 24 h, the ^1H NMR spectra indicated the regeneration of compounds **5a** and **5b**, with spectroscopic yields of 60% for compound **5a** and 46% for compound **5b**. We presumed that compounds **10a** and **10b** could also operate as pre-catalysts in transfer-hydrogenation reactions if the pyridine ligand was labile enough to temporarily set this moiety free for the catalytic cycle. Indeed, 6 mol% of a catalytic mixture of compound **10a** enabled the reduction of acetophenone at 77 °C in [D_8]2-propanol, with a conversion of 95% within 2.5 h and a TOF value of 6.4 h^{-1}; this catalytic performance was lower in comparison to the catalytic reduction of acetophenone with compound **5a** (1.2 mol%, 77 °C, TOF 133 h^{-1}). Compound **10b** showed only a modest conversion of 20% within 2.5 h (TOF 1.3 h^{-1}) and 76% within 23 h. Therefore, the best initial rhenium species for the catalysis of transfer-hydrogenation reactions are the bifunctional complexes **5a** and **5b**.

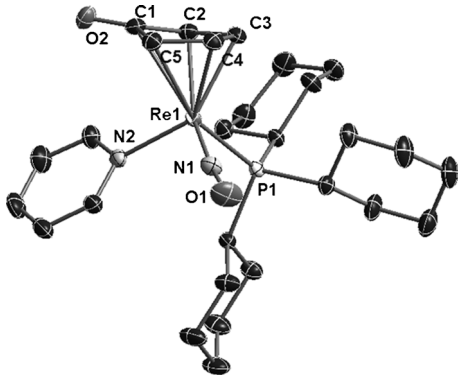

Figure 8. Molecular structure of compound **10b**. Thermal ellipsoids are set at 50% probability. All hydrogen atoms and solvent molecules are omitted for clarity. Selected bond lengths [Å] and angles [°]: Re1–N1 1.7638(15), Re1–N2 2.1540(14), Re1–P1 2.4084(4), N1–O1 1.2064(19), Re1–C1 2.5678(16), Re–C2 2.2914(16), Re–C3 2.2011(16), Re–C4 2.1796(16), Re–C5 2.2962(17), C1–O2 1.249(2), C1–C2 1.469(2), C2–C3 1.448(2), C3–C4 1.424(2), C4–C5 1.435(2), C5–C1 1.461(2); Re1-N1-O1 173.35(14), N1-Re1-P1 90.16(5), N1-Re1-N2 101.52(6), P1-Re1-N2 93.14(4).

Conclusion

Bifunctional rhenium catalysts of the type [Re(H)(NO)(L)-(C_5H_4OH)] (L = PCy_3 (**5a**), P*i*Pr_3 (**5b**)) were synthesized and showed partial isomerization into *trans*-dihydride species of the type [$Re(H)_2$(NO)(L)(C_5H_4O)] (**6a** and **6b**), which is atypical of bifunctional catalysts, with the apparent formation of strong Re–H bonds. These complexes were the basis for deuterium exchange reactions with D_2O and D_2 at the acidic H_O and hydridic H_{Re} atoms. DFT calculations supported the existence of stable *trans*-dihydride complexes and of a HOR-associated transition state (**TS3**) in the hydrogen-exchange reaction. Furthermore we demonstrated that compounds **5a** and **5b** performed well in the catalytic transfer hydrogenation reactions of ketones and imines, with some very good TOFs using 2-propanol. The catalytic activity was significantly influenced by the presence of primary alcohols, as well as by water. When pyridine was present in the catalytic solution, the 16e$^-$ cyclopentadienone complexes were trapped, thereby forming [Re(NO)(PR_3)(C_5H_4O)(py)] compounds (R = *i*Pr (**10a**), Cy (**10b**)). The 16e$^-$ intermediates that were generated from the loss of pyridine from compounds **10a** and **10b** (**E**) were unstable, which may be the cause for the observed catalyst degradation, especially when no donor ligands of any kind were available for stabilization. Compounds **10a** and **10b** were used as pre-catalysts in the transfer hydrogenation reactions, albeit with lower activities than compounds **5a** and **5b**, which remains a challenge to tune of the lability of this ligand. In summary, we have developed a new active Shvo-type transfer hydrogenation system that is based on the non-platinum-metal rhenium and contributes to the field of metal–ligand bifunctional catalysis.

Experimental Section

General: All operations were carried out by using Schlenk techniques or in a glove box (M. Braun 150 G-B) under a nitrogen atmosphere. The solvents were dried over sodium benzophenone (THF, Et_2O, hydrocarbons). The deuterated solvents that were used for NMR experiments were dried over sodium benzophenone (C_6D_6, [D_8]toluene, [D_8]THF) and vacuum transferred for storage in Schlenk flasks that were fitted with Teflon valves. 2-Propanol (dried over 3 Å molecular sieves) and [D_8]2-propanol were degassed three times and used without further purification. *tert*-Butyldimethylsilyl trifluoromethylsulfonate and cyclopentenone (Acros Organics) were purchased, degassed, and used without further purification. Substrates for catalysis were distilled before use (Fluka, Aldrich). NMR experiments were carried out on a Varian Gemini 300 and on Bruker DRX 500, AV2 500, and AV2 400 machines with 5 mm diameter NMR tubes that were equipped with Teflon valves, which allowed for degassing and the further introduction of gases into the samples. 1-(*tert*-Butyldimethylsiloxy) cyclopentadiene and [Re(NO)(H)(PR_3)$_2$(Br)] (**1a** and **1b**) were prepared according to literature procedures.[15b,32]

Preparation of the ligands and complexes: **($C_5H_4OSiMe_2tBu$)Li (2)**:[33] To a solution of 1-(*tert*-butyldimethylsiloxy) cyclopentadiene (33 mg, 0.169 mmol) in pentane, was added a solution of *n*BuLi (0.075 mL, 0.169 mmol, 1.6 M in *n*-hexane) and the solution was stored at −30 °C overnight. The solvent was removed, the precipitate was washed with pentane, and the solvent was evaporated in vacuo. The residual solid gave compound **2** as a white powder in about 95 % yield. ^{1}H NMR (200 MHz, [D$_8$]THF): δ = 5.25 (m, 2H; C_5H_4), 5.14 (m, 2H; C_5H_4), 0.93 (s, 9H; SiC(CH_3)$_3$), 0.07 ppm (s, 6H; Si(CH_3)$_2$); ^{13}C{^{1}H} NMR (50 MHz, [D$_8$]THF): δ = 140.1 (s; $C_{ipso}C_5H_4$), 97.4, 92.1 (s; C_5H_4), 28.4 (s; Si*C*(CH_3)$_3$), 18.9 (s; SiC(CH_3)$_3$), −4.1 ppm (s; Si(CH_3)$_2$).

[Re(H)(NO)(P*i*Pr$_3$)($C_5H_4OSiMe_2tBu$)] (3a): A mixture of compound **2** (55 mg, 1.75 equiv, 0.292 mmol) and [Re(H)(NO)(Br)(P*i*Pr$_3$)$_2$] (103 mg, 0.167 mmol) in THF (5 mL) was stirred for 2 h at room temperature to produce a dark orange color. The solvent was evaporated in vacuo and the product was extracted with pentane until the extracts were colorless. Yield of **3a**: 92–94 %; ^{1}H NMR (400 MHz, C_6D_6): δ = 4.64, 4.70 (m, 2H; C_5H_4), 2.02 (m, 3H; C*H*(CH_3)$_2$), 1.09–1.21 (m, 18H; PCH(CH_3)$_2$), 0.87 (s, 9H; SiC(CH_3)$_3$), 0.13 (s, 6H; Si(CH_3)$_2$), −9.01 ppm (d, 1H, ^2J(H,P) = 28.1 Hz; ReH); ^{13}C{^{1}H} NMR (100 MHz, C_6D_6): δ = 136.9 (s; $C_{ipso}C_5H_4$), 73.6, 72.8, 72.6, 72.1 (s; C_5H_4), 27.5, 27.3 (s; Si*C*H(CH_3)$_2$), 25.4 (s; SiC-(*C*H$_3$)$_3$), 20.3, 19.4 (s; PCH(*C*H$_3$)$_2$), 18.0 (s; Si*C*(CH_3)), −5.0, −5.2 ppm (s; Si(CH_3)$_2$); ^{31}P{^{1}H} NMR (162 MHz, C_6D_6): δ = 47.1 ppm (s; P*i*Pr$_3$); IR (ATR): $\tilde{\nu}$ = 2958, 2930, 2870 (CH), 1976 (ReH), 1629 cm^{-1} (NO); MS (ESI+): *m*/*z*: 574.2 [*M*+H]$^+$; elemental analysis calcd (%) for $C_{20}H_{41}NO_2PReSi$: C 41.94, H 7.21, N 2.45; found: C 42.27, H 7.28, N 2.27.

[Re(H)(NO)(PCy$_3$)($C_5H_4OSiMe_2tBu$)] (3b): A mixture of compound **2** (231 mg, 1.14 mmol) and [Re(H)(NO)(Br)(PCy$_3$)$_2$] (652 mg, 0.76 mmol) in THF (15 mL) was stirred for 2 h at room temperature to give a dark orange solution. The solvent was evaporated in vacuo and the product was extracted with pentane until the extracts were colorless. After drying in vacuo, compound **3b** was obtained in 86 % yield, along with minor amounts of free tricyclohexylphosphine. Crystallization from pentane at −30 °C over several days provided pure compound **3b** in 64 % yield. ^{1}H NMR (400 MHz, C_6D_6): δ = 4.83, 4.79, 4.64, 4.57 (m, 1H; C_5H_4), 2.12–1.16 (m, 33H; Cy), 0.90 (s, 9H; SiC(CH_3)$_3$), 0.21, 0.16 (s, 3H; Si(CH_3)$_2$), −8.97 ppm (d, 1H, ^2J(H,P) = 27.9 Hz; ReH); ^{13}C{^{1}H} NMR (100 MHz, C_6D_6): δ = 138.1 (s; CO), 74.7, 73.4, 72.9, 71.4 (s; C_5H_4), 38.2, 37.9, 31.3, 30.6 (s; Cy), 28.3, 28.3, 28.1 (s; SiC(*C*H$_3$)$_3$), 27.4, 26.0 (s; Cy), 18.6 (s; Si*C*-(CH$_3$)$_3$), −4.3, −4.5 ppm (s; Si(CH_3)$_2$); ^{31}P{^{1}H} NMR (162 MHz, C_6D_6): δ = 37.8 ppm (s; PCy$_3$); IR (ATR): $\tilde{\nu}$ = 2924, 2847 (CH), 1975 (ReH), 1620 cm^{-1} (NO); MS (ESI+): *m*/*z*: 694.3 [*M*+H]$^+$; elemental analysis calcd (%) for $C_{29}H_{53}NO_2PSiRe$: C 50.26, H 7.71, N 2.02; found: C 50.29, H 7.90, N 2.02.

[Re(H)(NO)(P*i*Pr$_3$)(C_5H_4O)][NBu$_4$] (4a): To a solution of compound **3a** (317 mg, 0.554 mmol) in THF (10 mL) was added TBAF (554 μL, 0.554 mmol, 1 M in THF). After the mixture had been stirred for 2 h at room temperature, the solvent was removed in vacuo and the residue was re-dissolved in toluene and filtered through celite. The solvent was removed in vacuo and compound **4a** was precipitated from a toluene/pentane mixture. After drying in vacuo, compound **4a** was obtained as an orange oil. Yield: 64 %; ^{1}H NMR (400 MHz, C_6D_6): δ = 5.56 (s, 1H; C_5H_4), 4.89 (s, 1H; C_5H_4), 4.56 (s, 1H; C_5H_4), 3.27 (s, 1H; C_5H_4), 3.19 (m; N(C*H*$_2$(CH$_2$)$_2$CH$_3$)$_4$), 2.61 (m, 3H; PC*H*(CH_3)$_2$), 1.48–1.34 (m; PCH-(C*H*$_3$)$_2$ and NC*H*$_2$(CH$_2$)$_2$(CH$_3$)), 0.95 (m; N(CH$_2$(CH$_2$)$_2$C*H*$_3$)$_4$), −8.01 ppm (d, 1H, ^2J(H,P) = 23.0 Hz; ReH); ^{13}C{^{1}H} NMR (100 MHz, C_6D_6): δ = 167.5 (s; CO), 68.8, 66.1, 65.2, 64.7 (s; C_5H_4), 58.8 (s, CH$_2$-(NBu$_4$)), 26.2, 26.0 (s; P*C*H(CH_3)$_2$), 24.5 (s; CH$_2$(NBu$_4$)), 21.7 (s; CH$_2$-(NBu$_4$)), 20.5, 20.2 (s; PCH(*C*H$_3$)$_2$), 14.3 ppm (s; CH$_3$, (NBu$_4$)); ^{31}P{^{1}H} NMR (162 MHz, C_6D_6): δ = 43.3 (s; P*i*Pr$_3$); IR (ATR): $\tilde{\nu}$ = 2957, 2929, 2869 (CH), 1934 (ReH), 1533 cm^{-1} (NO); MS (ESI−): *m*/*z*: 458.4 [*M*]$^-$; elemental analysis calcd (%) for $C_{30}H_{62}N_2O_2PRe$: C 51.47, H 8.93, N 4.00; found: C 51.39, H 8.95, N 3.92.

[Re(H)(NO)(PCy$_3$)(C_5H_4O)][NBu$_4$] (4b): To a solution of compound **3b** in THF (10 mL) containing free PCy$_3$ (312 mg, 0.321 mmol) was added TBAF (321 μL, 0.321 mmol, 1 M in THF). After the mixture had been stirred for 2 h at room temperature, the solvent was removed in vacuo. The residue was washed with pentane to remove free PCy$_3$. and compound **4b** was precipitated from Et$_2$O and excess of pentane. The precipitate was dried in vacuo to give an orange oil. Yield: 85 %; ^{1}H NMR (400 MHz, C_6D_6): δ = 5.52, 4.83, 4.56, 3.25 (m, 1H; C_5H_4), 3.26 (m; N-(C*H*$_2$(CH$_2$)$_2$CH$_3$)$_4$), 2.44–1.74 (m, 33H; Cy), 1.51, 1.38 (m; N(CH$_2$-(C*H*$_2$)$_2$CH$_3$)$_4$), 0.98 (m; N(CH$_2$(CH$_2$)$_2$C*H*$_3$)$_4$), −8.11 ppm (d, 1H, ^2J-(H,P) = 22.8 Hz; ReH); ^{13}C{^{1}H} NMR (100 MHz, C_6D_6): δ = 167.2 (s; CO), 67.9, 65.5, 64.7 63.9 (s; C_5H_4), 58.3 (s; CH$_2$(NBu$_4$), 35.7, 35.5, 31.5, 30.0, 28.1, 27.5 (s; Cy), 24.1, 19.9 (s; CH$_2$(NBu$_4$)), 13.8 ppm (s; CH$_3$-(NBu$_4$)); ^{31}P{^{1}H} NMR (162 MHz, C_6D_6): δ = 31.7 ppm (s; PCy$_3$); IR (ATR): $\tilde{\nu}$ = 2958, 2853 (CH, N(Bu)$_4$), 2925, 2872 (CH, Cy), 1958 (ReH), 1533 cm^{-1} (NO); MS (ESI−): *m*/*z*: 578.4 [*M*]$^-$; elemental analysis calcd (%) for $C_{39}H_{74}N_2O_2PRe$: C 57.11, H 9.09, N 3.42; found: C 57.04, H 9.15, N 3.40.

[Re(H)(NO)(P*i*Pr$_3$)(C_5H_4OH)] (5a): An excess of ammonium bromide was added to a solution of compound **4a** (483 mg, 0.60 mmol) in THF (15 mL) and the mixture was stirred overnight. The solvent was removed in vacuo and the residue was dissolved in toluene and filtered over celite. The solvent was removed in vacuo and the product was purified by column chromatography on silica gel (Et$_2$O/THF, 7:1) at −30 °C to obtain compound **5a** as a yellow solid. Yield: 51 %; MS (ESI−): *m*/*z*: 458.4 [*M*]$^-$; elemental analysis calcd (%) for $C_{14}H_{27}NO_2PRe$: C 36.67, H 5.93, N 3.05; found: C 36.78, H 5.99, N 3.00. ^{1}H NMR (400 MHz, [D$_8$]THF): δ = 8.03 (br s, 1H; OH), 4.80 (m, 1H; C_5H_4), 4.77 (m, 1H; C_5H_4), 4.66 (m, 1H; C_5H_4), 4.62 (m, 1H; C_5H_4), 2.13 (m, 3H; PC*H*(CH_3)$_2$), 1.16 (m, 18H; PCH(C*H*$_3$)$_2$), −9.42 ppm (d, 1H, ^2J(H,P) = 27.4 Hz; ReH); ^{13}C{^{1}H} NMR (100 MHz, [D$_8$]THF): δ = 141.1 (s; $C_{ipso}C_5H_4$), 72.1 (s, 2C; C_5H_4), 71.7, 70.5 (s; C_5H_4), 28.1, 27.9 (s; P*C*H(CH_3)$_2$), 20.4, 19.5 ppm (s; PCH(*C*H$_3$)$_2$); ^{31}P{^{1}H} NMR (162 MHz, [D$_8$]THF): δ = 47.8 ppm (s; P*i*Pr$_3$); ^{1}H NMR (500 MHz, C_6D_6): δ = 9.20 (br s, 1H; OH), 5.26 (s, 1H; C_5H_4), 4.82 (s, 1H; C_5H_4), 4.62 (s, 1H; C_5H_4), 4.58 (s, 1H; C_5H_4), 2.00 (m, 3H; PC*H*(CH_3)$_2$), 1.22–1.08 (m, 18H; PCH(C*H*$_3$)$_2$), −8.76 ppm (d, 1H, ^2J-(H,P) = 27.2 Hz; ReH); ^{13}C{^{1}H} NMR (125.8 MHz, C_6D_6): δ = 142.0 (s; $C_{ipso}C_5H_4$), 73.1, 71.6, 70.9, 67.9 (s; C_5H_4), 28.1, 27.9 (s; P*C*H(CH_3)$_2$), 20.6, 19.7 ppm (s; PCH(*C*H$_3$)$_2$); ^{31}P{^{1}H} NMR (202.5 MHz, C_6D_6): δ = 48.1 ppm (s; P*i*Pr$_3$); IR (ATR): $\tilde{\nu}$ = 3118 (br; OH), 2960, 2922, 2909, 2868 (CH), 2009 (ReH), 1607 cm^{-1} (NO).

[(C_5H_4O)Re(NO)(PiPr$_3$)(H)$_2$] (6a): ^{1}H NMR (500 MHz, C_6D_6): δ = 4.87 (m, 2H; C_5H_4), 4.45 (br s, 2H; C_5H_4), 1.86 (m, 3H; PC*H*(CH_3)$_2$), 0.90 (m, 18H; PCH(C*H*$_3$)$_2$), −3.43 ppm (d, 2H, ^2J(H,P) = 46.7 Hz; ReH); ^{13}C{^{1}H} NMR (125.8 MHz, C_6D_6): δ = 175.0 (s; CO), 82.3, 68.5 (s, 2C; C_5H_4), 28.5, 28.2 (s; P*C*H(CH_3)$_2$), 19.2, 19.2 ppm (s; PCH(*C*H$_3$)$_2$); ^{31}P{^{1}H} NMR (202.5 MHz, C_6D_6): δ = 52.3 ppm (s; P*i*Pr$_3$); IR (ATR): $\tilde{\nu}$ = 2960, 2922, 2909, 2868 (CH), 2218, 2079 (ReH), 1736, 1713 cm^{-1} (NO/CO).

[Re(H)(NO)(PCy$_3$)(C_5H_4OH)] (5b): An excess of ammonium bromide (425 mg, 4.34 mmol) was added to a solution of compound **4b** (178 mg, 0.217 mmol) in THF (15 mL) and stirred overnight. The solvent was removed in vacuo and the residue was dissolved in toluene and filtered through celite. The solvent was removed in vacuo and the product was purified by column chromatography on silica gel (Et$_2$O/THF, 7:1) at −30 °C and compound **5b** was obtained as a yellow solid. Yield: 54 %; MS (ESI−): *m*/*z*: 578.3 [*M*]$^-$; elemental analysis calcd (%) for $C_{23}H_{39}NO_2PRe$: C 47.73, H 6.79, N 2.42; found: C 48.00, H 6.87, N 2.23. ^{1}H NMR (400 MHz, [D$_8$]THF): δ = 8.03 (s, 1H; OH), 4.88 (m, 2H; C_5H_4), 4.65 (m, 1H; C_5H_4), 4.58 (m, 1H; C_5H_4), 1.98–1.26 (m; Cy), −9.48 ppm (d, 1H; ^2J(H,P) = 27.4 Hz; ReH); ^{13}C{^{1}H} NMR (100 MHz, [D$_8$]THF): δ = 140.4 (s; CO), 71.7, 71.7, 71.2, 70.2 (s; C_5H_4OH), 37.5, 37.2, 30.4, 29.8, 27.6, 26.7 ppm (s; Cy); ^{31}P{^{1}H} NMR (162 MHz, [D$_8$]THF): δ = 36.5 ppm (s; PCy$_3$); ^{1}H NMR (400 MHz, C_6D_6): δ = 6.71 (br s, 1H; OH), 4.96 (m, 1H; C_5H_4), 4.66 (m, 2H; C_5H_4), 4.34 (m, 1H; C_5H_4), 2.18–1.15 (m; Cy), −8.82 ppm (d, 1H; ^2J(H,P) = 26.9 Hz; ReH); ^{13}C{^{1}H} NMR (100 MHz, C_6D_6): δ = 141.2 (s; $C_{ipso}C_5H_4$), 73.4, 72.4, 71.3, 68.2 (s; C_5H_4), 38.4, 38.2, 31.3, 30.6, 27.5, 26.8 ppm (s; Cy); ^{31}P{^{1}H} NMR (162 MHz, C_6D_6): δ = 37.0 ppm (s; PCy$_3$). IR (ATR): $\tilde{\nu}$ = 3144 (OH), 2924, 2848 (CH), 2005 (ReH), 1620 cm^{-1} (NO).

[(C_5H_4O)Re(NO)(PCy$_3$)(H)$_2$] (6b): ^{1}H NMR (400 MHz, C_6D_6): δ = 5.14, 4.89 (m, 4H; C_5H_4), 2.18–1.15 (m; Cy), −3.14 ppm (d, 2H; ^2J(H,P) = 47.0 Hz; ReH); ^{13}C{^{1}H} NMR (100 MHz, C_6D_6): δ = 181.6 (s; CO), 82.6,

68.5 (s, 2C; C_5H_4), 38.7, 30.1, 28.3, 28.2, 27.8, 27.7 ppm (s; Cy); $^{31}P\{^1H\}$ NMR (162 MHz, C_6D_6): $\delta = 41.6$ ppm (s; PCy_3); IR (ATR): $\tilde{\nu} =$ 2923, 2850 (CH), 2205, 2021 (ReH), 1712 cm^{-1} (NO).

[Re(NO)(P*i*Pr$_3$)(pyridine)(cyclopentadienone)] (10a): Compound **5a** (10 mg, 0.0218 mmol) was dissolved in 2-propanol (5 mL) and an excess of pyridine (175.6 μL, 2.18 mmol) and the substrate (4.36 mmol) were added. The solution was stirred overnight at 80 °C and the solvent was removed in vacuo. The residue was washed several times with pentane. Compound **10a** was obtained as an orange-red solid in 56% yield. ^1H NMR (400 MHz, CD_3CN): $\delta = 8.67$ (d, 2H; *o*-CH), 7.63 (t, 1H; *p*-CH), 7.25 (t, 2H; *m*-CH), 6.07, 4.47, 4.26, 3.26 (m, 1H; C_5H_4O), 2.45–2.36 (m, 3H; PC*H*$(CH_3)_2$), 1.22–1.15 ppm (m, 18H; PCH$(CH_3)_2$); $^{13}C\{^1H\}$ NMR (100 MHz, CD_3CN): $\delta = 171.4$ (s; CO), 156.6 (s, 2C; *o*-CH), 137.3 (s; *p*-CH), 126.1 (s, 2C; *m*-CH), 77.6, 75.1 (s, 2C; C_5H_4), 28.6, 28.3 (s; P*C*H$(CH_3)_2$), 20.2, 19.6 ppm (s; PCH$(CH_3)_2$); $^{31}P\{^1H\}$ NMR (162 MHz, CD_3CN): $\delta = 21.8$ (s; P*i*Pr$_3$); IR (ATR): $\tilde{\nu} = 2963$, 2931, 2873 (CH), 1625, 1584 cm^{-1} (NO/CO); MS (ESI): *m*/*z*: 537.2 [*M*+H]; elemental analysis calcd (%) for $C_{19}H_{30}N_2O_2PRe$: C 42.60, H 5.65, N 5.23; found: C 42.23, H 5.56, N 5.16.

[Re(NO)(PCy$_3$)(pyridine)(cyclopentadienone)] (10b): Compound **5b** (10 mg, 0.0218 mmol) was dissolved in 2-propanol (5 mL) and an excess of pyridine (175,6 μL, 2.18 mmol) and the substrate (4.36 mmol) were added. The solution was stirred overnight at 80 °C and the solvent was removed in vacuo. Compound **10b** was precipitated from a THF and excess of pentane solution and, after drying, compound **10b** was obtained as a yellow solid in 68% yield. ^1H NMR (400 MHz, CD_3CN): $\delta = 8.56$ (d, 2H; *o*-CH), 7.58 (t, 1H; *p*-CH), 7.17 (t, 2H; *m*-CH), 6.00 (m, 1H; C_5H_4O), 4.30 (m, 1H; C_5H_4O), 4.22 (m, 1H; C_5H_4O), 3.23 (m, 1H; C_5H_4O), 2.08–1.16 ppm (m; Cy); $^{13}C\{^1H\}$ NMR (100 MHz, CD_3CN): $\delta =$ 170.6 (s; CO), 156.2 (s, 2C; *o*-CH), 136.7 (s; *p*-CH), 125.7 (s, 2C; *m*-CH), 76.9, 73.9 (s, 2C; C_5H_4), 37.9, 37.6, 30.3, 29.6, 27.8 ppm (s; Cy); $^{31}P\{^1H\}$ NMR (162 MHz, CD_3CN): $\delta = 12.6$ ppm (s; PCy_3); IR (ATR): $\tilde{\nu} =$ 2928, 2847 (CH), 1629, 1568 cm^{-1} (NO/CO); MS (ESI): *m*/*z*: 657.3 [*M*+H]; elemental analysis calcd (%) for $C_{28}H_{43}N_2O_2PRe$: C 51.20, H 6.60, N 4.26; found: C 50.98, H 6.49, N 4.08.

[Re(D)(NO)(PR$_3$)(C_5H_4OD)]: *Method A (D_2O)*: Rhenium hydride **5a**/**5b** was dissolved in [D_8]THF (0.4 mL) in a Young NMR tube that was fitted with a Teflon valve. An excess of D_2O (100 equiv) was added and the mixture was shaken over a period of 5 h at room temperature to afford 94% H/D exchange for compound **5a** and 92% for compound **5b**.

Method B (D_2): Rhenium hydride **5a**/**5b** was dissolved in [D_8]THF (0.4 mL) in a Young NMR tube that was fitted with a Teflon valve. The NMR tube was degassed by three freeze-pump-thaw cycles and filled with D_2 (1.5 bar). The disappearance of the hydride signal was monitored by ^1H NMR spectroscopy as a function of time. After 77 h, the H_{Re} exchange was 85% for compound **5a** and 55% for compound **5b**.

Computational methods: DFT calculations on freely optimized PMe_3-substituted model compounds (**A**–**E**) and on the transition states (**TS1**–**TS5**) were carried out by employing the B3LYP[22] functional and the 6–31G(d,p)[23] basis set for H to P and the LANL2DZ[24] basis set in connection with the associated effective core potential for Re with the GAMESS program package.[25] All free energies were calculated at 298.15 K and referenced to the energy of structure $\mathbf{A_1}$.

X-ray diffraction: Single-crystal X-ray diffraction data were collected at 183(2) K on an Xcalibur diffractometer (Agilent Technologies, Ruby CCD detector) for all compounds by using a single-wavelength Enhance X-ray source with $Mo_{K\alpha}$ radiation ($\lambda = 0.71073$ Å).[34] Suitable single crystals were mounted by using polybutene oil on the top of a glass fiber that was fixed on a goniometer head and immediately transferred into the diffractometer. Pre-experimental-, data-collection-, data-reduction-, and analytical-[35] or semi-empirical absorption corrections were performed with the program suite CrysAlisPro.[36] The crystal structures were solved with SHELXS97[37] using direct methods. The structure refinements were performed by full-matrix least-squares on F2 with SHELXL97.[37] All programs used during the crystal structure determination process are included in the WINGX software.[38] PLATON[39] was used to check the result of the X-ray analyses. CCDC-854668 (**3a**), CCDC-854669 (**3b**), CCDC-854670 (**5a**), and CCDC-854671 (**10b**) contain the supplementary crystallographic data for this paper. These data can be obtained free of charge from The Cambridge Crystallographic Data Centre via www.ccdc.cam.ac.uk/data_request/cif.

In the crystal structures of compounds **3a** and **3b**, artefactual electron density was observed near the heavy-atom sites (less than 0.8 Å). Different types of absorption correction were tried but without significant improvements. In the crystal structure of compound **10b**, THF solvent molecules co-crystallized with the metal–organic species in a ratio 2:1. One of these solvent molecules was disordered over two sets of positions with a site-occupancy factor of 0.5. The hydride atoms in compounds **3a**, **3b**, and **5a**, and the H atom of the hydroxy group in compound **5a** were located in difference Fourier maps and freely refined. All other hydrogen positions were calculated after each cycle of refinement using a riding model, with C–H = 0.93 Å and $U_{iso}(H) = 1.2U_{eq}(C)$ for aromatic H atoms, C–H = 0.97 Å and $U_{iso}(H) = 1.2U_{eq}(C)$ for methylene H atoms, C–H = 0.98 Å and $U_{iso}(H) = 1.2U_{eq}(C)$ for methine H atoms, and C–H = 0.96 Å and $U_{iso}(H) = 1.5U_{eq}(C)$ for methyl H atoms.

Kinetic studies: Kinetic studies were carried out in an NMR tube that was fitted with a Young Teflon valve. The complex (0.00218 mmol) was dissolved in [D_8]2-propanol (0.4 mL) and acetophenone (0.1823 mmol) or benzaldehyde (0.218 mmol) were added. The disappearance of acetophenone was monitored by ^1H NMR spectroscopy as a function of time at 350 K.

Catalytic reduction: All catalysis was carried out in Schlenk flasks that were fitted with Teflon valves. Compound **5a** (0.00128 mmol) and substrate (0.436 mmol) were mixed in 2-propanol (1 mL, 30 equiv) and the mixture was heated at 120 °C. After an appropriate reaction time, an aliquot of the reaction mixture was diluted in pentane and filtered through celite to remove the catalyst. The products were identified and the yields were determined by GCMS analysis (r.t. = retention time).

PhCO(CH_3): r.t. = 6.55 min, *m*/*z* 120; PhCHOH(CH_3): r.t. = 6.47 min, *m*/*z* 122; PhCO(CH_2CH_3): r.t. = 8.06 min, *m*/*z* 134; PhCHOH(CH_2CH_3): r.t. = 7.84 min, *m*/*z* 136; PhCOPh: r.t. = 11.27 min, *m*/*z* 182; PhCHOHPh: r.t. = 11.20 min, *m*/*z* 184; *p*-FPhCOPh-*p*F: r.t. = 5.52 min, *m*/*z* 218; *p*-FPhCHOHPh-*p*F: r.t. = 4.98 min, *m*/*z* 220; $CH_3CO(C(CH_3)_3)$: r.t. = 2.59 min, *m*/*z* 100; $CH_3CHOH(C(CH_3)_3)$: r.t. = 3.10 min, *m*/*z* 102; C_5H_8O: r.t. = 4.29 min, *m*/*z* 84; C_5H_9OH: r.t. = 4.14 min, *m*/*z* 86; $CH_3COPhCOCH_3$: r.t. = 9.06 min, *m*/*z* 162; $CH_3CHOHPhCOCH_3$: r.t. = 9.56 min, *m*/*z* 164; $CH_3CHOHPhCHOHCH_3$: r.t. = 9.21 min, *m*/*z* 166; C_6H_{10}: r.t. = 2.26 min, *m*/*z* 82; C_6H_{12}: r.t. = 2.09 min, *m*/*z* 84; PhCHNPh: r.t. = 9.093, *m*/*z* 181; $PhCH_2NHPh$: r.t. = 9.355, *m*/*z* 183; *p*-ClPhCHNPh-*p*Cl: r.t. = 9.779, *m*/*z* 249; *p*-$ClPhCH_2NHPh$-*p*Cl: r.t. = 10.235, *m*/*z* 251; PhCHN(α-naphtyl): r.t. = 10.513, *m*/*z* 231; $PhCH_2NH$(α-naphtyl): r.t. = 10.683, *m*/*z* 233.

Acknowledgements

We thank the Swiss National Science Foundation and the University Zurich for financial support.

[1] a) Y. Shvo, D. Czarkie, *J. Organomet. Chem.* **1986**, *315*, C25; b) Y. Blum, D. Czarkie, Y. Rahamim, Y. Shvo, *Organometallics* **1985**, *4*, 1459; c) B. L. Conley, M. K. Pennington-Boggio, E. Boz, T. J. Williams, *Chem. Rev.* **2010**, *110*, 2294.

[2] Y. Shvo, I. Goldberg, D. Czerkie, D. Reshef, Z. Stein, *Organometallics* **1997**, *16*, 133.

[3] a) J. S. M. Samec, J. E. Bäckvall, *Chem. Eur. J.* **2002**, *8*, 2955; b) C. P. Casey, G. A. Bikzhanova, Q. Cui, I. A. Guzei, *J. Am. Chem. Soc.* **2005**, *127*, 14062.

[4] a) C. P. Casey, S. W. Singer, D. R. Powell, R. K. Hayashi, M. Kavana, *J. Am. Chem. Soc.* **2001**, *123*, 1090; b) N. Menashe, Y. Shvo, *Organometallics* **1991**, *10*, 3885; c) N. Menashe, E. Salant, Y. Shvo, *J. Organomet. Chem.* **1996**, *514*, 97.

[5] a) L. Koren-Selfridge, H. N. Londino, J. K. Vellucci, B. J. Simmons, C. P. Casey, T. B. Clark, *Organometallics* **2009**, *28*, 2085; b) C. P.

Casey, T. E. Vos, G. A. Bikzhanova, *Organometallics* **2003**, *22*, 901; c) C. P. Casey, N. A. Strotman, S. E. Beetner, J. B. Johnson, D. C. Priebe, T. E. Vos, B. Khodavandi, I. A. Guzei, *Organometallics* **2006**, *25*, 1230; d) C. P. Casey, N. A. Strotman, S. E. Beetner, J. B. Johnson, D. C. Priebe, I. A. Guzei, *Organometallics* **2006**, *25*, 1236.

[6] a) S. Hashiguchi, A. Fujii, J. Takehara, T. Ikariya, R. Noyori, *J. Am. Chem. Soc.* **1995**, *117*, 7562; b) J. X. Gao, T. Ikariya, R. Noyori, *Organometallics* **1996**, *15*, 1087; c) T. Ikariya, K. Murata, R. Noyori, *Org. Biomol. Chem.* **2006**, *4*, 393; d) R. Noyori, S. Hashiguchi, *Acc. Chem. Res.* **1997**, *30*, 97.

[7] a) H. H. Zhang, D. Z. Chen, Y. H. Zhang, G. Q. Zhang, J. B. Liu, *Dalton Trans.* **2010**, *39*, 1972; b) J. B. Johnson, J. E. Bäckvall, *J. Org. Chem.* **2003**, *68*, 7681; c) C. P. Casey, H. R. Guan, *J. Am. Chem. Soc.* **2009**, *131*, 2499; d) A. Comas-Vives, G. Ujaque, A. Lledos, *Organometallics* **2007**, *26*, 4135.

[8] H. Berke, *ChemPhysChem* **2010**, *11*, 1837.

[9] a) X. F. Wu, D. Vinci, T. Ikariya, J. L. Xiao, *Chem. Commun.* **2005**, 4447; b) K. Murata, T. Ikariya, *J. Org. Chem.* **1999**, *64*, 2186.

[10] a) X. W. Li, P. Chen, J. W. Faller, R. H. Crabtree, *Organometallics* **2005**, *24*, 4810; b) X. F. Wu, J. K. Liu, X. H. Li, A. Zanotti-Gerosa, F. Hancock, D. Vinci, J. W. Ruan, J. L. Xiao, *Angew. Chem.* **2006**, *118*, 6870; *Angew. Chem. Int. Ed.* **2006**, *45*, 6718.

[11] J. Washington, R. Mcdonald, J. Takats, N. Menashe, D. Reshef, Y. Shvo, *Organometallics* **1995**, *14*, 3996.

[12] a) C. P. Casey, H. R. Guan, *J. Am. Chem. Soc.* **2007**, *129*, 5816; b) R. M. Bullock, *Angew. Chem.* **2007**, *119*, 7504; *Angew. Chem. Int. Ed.* **2007**, *46*, 7360; c) M. G. Coleman, A. N. Brown, B. A. Bolton, H. R. Guan, *Adv. Synth. Catal.* **2010**, *352*, 967.

[13] Z. L. Chen, I. Timokhin, H. W. Schmalle, T. Fox, O. Blacque, H. Berke, *Eur. J. Inorg. Chem.* **2009**, 4119.

[14] A. Choualeb, A. J. Lough, D. G. Gusev, *Organometallics* **2007**, *26*, 3509.

[15] a) A. Choualeb, E. Maccaroni, O. Blacque, H. W. Schmalle, H. Berke, *Organometallics* **2008**, *27*, 3474; b) Y. Jiang, O. Blacque, T. Fox, C. M. Frech, H. Berke, *Chem. Eur. J.* **2009**, *15*, 3039.

[16] a) Y. F. Jiang, O. Blacque, T. Fox, C. M. Frech, H. Berke, *Organometallics* **2009**, *28*, 5493; b) X. Y. Liu, K. Venkatesan, H. W. Schmalle, H. Berke, *Organometallics* **2004**, *23*, 3153; c) B. Dudle, K. Rajesh, O. Blacque, H. Berke, *J. Am. Chem. Soc.* **2011**, *133*, 8168.

[17] a) G. W. Stowell, R. R. Whittle, C. M. Whaley, D. P. White, *Organometallics* **2001**, *20*, 1050; b) B. Machura, *Coord. Chem. Rev.* **2005**, *249*, 2277.

[18] C. A. Tolman, *Chem. Rev.* **1977**, *77*, 313.

[19] a) N. V. Belkova, E. S. Shubina, A. V. Ionidis, L. M. Epstein, H. Jacobsen, A. Messmer, H. Berke, *Inorg. Chem.* **1997**, *36*, 1522; b) A. Messmer, H. Jacobsen, H. Berke, *Chem. Eur. J.* **1999**, *5*, 3341; c) G. J. Kubas, *Chem. Rev.* **2007**, *107*, 4152.

[20] a) D. M. Heinekey, A. Lledos, J. M. Lluch, *Chem. Soc. Rev.* **2004**, *33*, 175; b) D. G. Hamilton, R. H. Crabtree, *J. Am. Chem. Soc.* **1988**, *110*, 4126.

[21] C. P. Casey, J. B. Johnson, S. W. Singer, Q. Cui, *J. Am. Chem. Soc.* **2005**, *127*, 3100.

[22] a) A. D. Becke, *J. Chem. Phys.* **1993**, *98*, 5648; b) P. J. Stephens, F. J. Devlin, C. F. Chabalowski, M. J. Frisch, *J Phys Chem. Us.* **1994**, *98*, 11623; c) C. T. Lee, W. T. Yang, R. G. Parr, *Phys. Rev. B* **1988**, *37*, 785.

[23] a) W. J. Hehre, Ditchfie. R, J. A. Pople, *J. Chem. Phys.* **1972**, *56*, 2257; b) J. D. Dill, J. A. Pople, *J. Chem. Phys.* **1975**, *62*, 2921; c) M. M. Francl, W. J. Pietro, W. J. Hehre, J. S. Binkley, M. S. Gordon, D. J. Defrees, J. A. Pople, *J. Chem. Phys.* **1982**, *77*, 3654.

[24] P. J. Hay, W. R. Wadt, *J. Chem. Phys.* **1985**, *82*, 270.

[25] M. W. Schmidt, K. K. Baldridge, J. A. Boatz, S. T. Elbert, M. S. Gordon, J. H. Jensen, S. Koseki, N. Matsunaga, K. A. Nguyen, S. J. Su, T. L. Windus, M. Dupuis, J. A. Montgomery, *J. Comput. Chem.* **1993**, *14*, 1347.

[26] T. A. Albright, J. K. Burdett, M. H. Whangbo, *Orbital Interactions in Chemistry*, Wiley, New York, **1985**.

[27] G. J. Kubas, in *Metal dihydrogen and σ-band complexes*, 1st ed., Kluwer Academic, New York, **2000**.

[28] M. Ito, T. Ikariya, *Chem. Commun.* **2007**, 5134.

[29] A. Berkessel, H. Gröger, *Asymmetric Organocatalysis: from Biomimetic Concepts to Applications in Asymmetric Synthesis*, Wiley-VCH, Weinheim, **2005**.

[30] D. R. Lide, *Handbook of Chemistry and Physics*, 73th ed., CRC Press, Boca Raton, FL, **1993**.

[31] S. Kozuch, S. Shaik, *Acc. Chem. Res.* **2011**, *44*, 101.

[32] a) H. Plenio, C. Aberle, *Organometallics* **1997**, *16*, 5950; b) H. Plenio, A. Warnecke, *Organometallics* **1996**, *15*, 5066.

[33] WO 01/53362 A1; US 6, 815,514 B2.

[34] Agilent Technologies (formerly Oxford Diffraction), Yarnton, England, **2011**.

[35] R. C. Clark, J. S. Reid, *Acta Crystallogr. Sect. A* **1995**, *51*, 887.

[36] *CrysAlisPro* (Versions 1.171.33.34d/1.171.35.11), Agilent Technologies (formerly Oxford Diffraction), Yarnton, England, **2011**.

[37] G. M. Sheldrick, *Acta Crystallogr. Sect. A* **2008**, *64*, 112.

[38] L. J. Farrugia, *J. Appl. Crystallogr.* **1999**, *32*, 837.

[39] A. L. Spek, *J. Appl. Crystallogr.* **2003**, *36*, 7.

Received: November 23, 2011
Published online: March 27, 2012

